ADAPTIVE PARTIAL DIFFERENTIAL EQUATION METHODS FOR OPTION PRICING

by

Guanghuan Hou

B.Sc., Zhejiang University, 2004

A PROJECT SUBMITTED IN PARTIAL FULFILLMENT
OF THE REQUIREMENTS FOR THE DEGREE OF
MASTER OF SCIENCE
in the Department
of
Mathematics

SIMON FRASER UNIVERSITY
Summer 2008

APPROVAL

Name: Guanghuan Hou

Degree: Master of Science

Title of project: Adaptive Partial Differential Equation Methods for Option Pricing

Examining Committee:

Dr. Robert Russell, Professor
Mathematics, Simon Fraser University
Senior Supervisor

Dr. Adam Oberman, Assistant Professor
Mathematics, Simon Fraser University
Co-Supervisor

Date Approved: _____

Abstract

This project investigates the application of finite difference schemes to option pricing problems. In particular, an adaptive mesh method is introduced to deal with difficulties that arise in the numerical approximation of PDE's in the presence of discontinuities, such as a barrier. Compared to an equidistant mesh, this adaptive mesh method substantially increases the numerical accuracy with the same number of grid points. Several finite difference schemes for pricing American options are studied and compared both in the one dimensional and two dimensional case. The behaviors of the price and hedge factors of various types of barrier options and American barrier options are further studied in detail.

Acknowledgments

I would like to thank my supervisor, Dr. Robert Russell; I have benefited greatly from his considerable help and guidance. I also thank Dr. Adam Oberman for supervising my project. Special thanks to Dr. Satish Reddy for his helpful advice during the research and writing of this project. Thanks also to Dr. Gary Parker and Dr. Rachel Kuske for their helpful advice. Important feedback has also been provided by Bryan Quaife, Jingtang Ma and Xiangmin Xu at various stages of this project. Thanks to all the members of the PIMS lab; you have always been there when needed. I also want to thank all my friends in Vancouver, who make my life here enjoyable. Last, and certainly not least, thanks to my parents for their support and encouragement.

Guanghuan Hou
Simon Fraser University
Summer 2008

Contents

List of Tables

List of Figures

Chapter 1

Introduction

1.1 Background

Over last three decades, the trading of options has grown dramatically, and now huge volumes of options, worth many billions of currency units, are traded daily on global exchanges (such as the Korea Stock Exchange, Chicago Board Options Exchange, MONEP, Eurex and American Stock Exchange) [9], and over the counter by banks and financial institutions. Therefore, option pricing has become increasingly important in the financial world.

Definition: An European option [24] gives the holder the right, but not the obligation, to buy or sell an underlying asset on a date T in the future. A call option is the right to buy at a strike price K and has a payoff of $\max(S - K, 0)$. The 0 corresponds to the scenario where the option holder does not exercise their right to buy. A European put option, with the same strike price, has payoff $\min(K - S, 0)$. For example, trader A purchases a call option to buy 1 share of XYZ Corp from trader B at \$50/share. If the share price of XYZ stock rises to \$60/share at T, then trader A can exercise the call and buy 1 share for \$50 from trader B and sell it at \$60 in the stock market, reflecting a profit of \$10. If the share price of XYZ Corp is below \$50 at T, then there is no point exercising a call option and it has value \$0. Since the option buyer obtains certain rights, the buyer must pay a premium for these rights, usually when the contract is initiated. The goal of option pricing is to determine a fair market value for this premium.

Various Types of Options: An European option can be exercised only at the maturity date T. American options can be exercised at any time $t \leq T$. A Bermudan option [40] can be exercised at a finite set of dates $t_i \leq T$. A barrier option [37] is activated (knocked in)

or extinguished (knocked out) when the price of the underlying asset crosses a certain level (called a barrier). For example, an up-and-out barrier call option gives the option holder the payoff of a call option if the price of the underlying asset does not reach a higher barrier level before the expiration date. More complicated barrier options may have two barriers (double barrier options). As well as barrier options, many exotic options present discontinuities. For example, a digital option [37] is characterized by a payoff equal to $1(l < S < u)$ where 1 stands for the indicator function of the set A.

1.1.1 Brownian Motion

In 1973, Fischer Black and Myron Scholes published their seminal paper 'The Pricing of Options and Corporate Liabilities' [1], which derived the Black-Scholes Equation by assuming that the underlying assets follows a geometric Brownian motion (GBM) process. The returns on the assets are governed by the stochastic differential equation (SDE)

$$\frac{dS_t}{S_t} = \mu dt + \sigma dW_t, \tag{1.1}$$

where S_t is the price of the underlying asset at time t, μ is the constant expected return of the asset, and σ is the constant volatility of asset returns. Moreover, W_t is a Wiener process, or Brownian motion. The GBM process can be relaxed for other processes such as CEV or a mean-reverting process, although greater attention will be required in correctly choosing the numerical method [37].

1.2 Black-Scholes Equation

This section lists a few forms of Black-Scholes equations.
Assuming an equity S follows geometric Brownian motion, the Black-Scholes equation [1] was derived as

$$\frac{\partial V}{\partial t} + \frac{1}{2}\sigma^2 S^2 \frac{\partial^2 V}{\partial S^2} + rS\frac{\partial V}{\partial S} - rV = 0. \tag{1.2}$$

with initial condition

$$V(S,T) = \begin{cases} \max(S-K,0) \text{ Call}, \\ \max(K-S,0) \text{ Put}, \end{cases} \tag{1.3}$$

where V is the option (call, put) value, K is the strike price, r is the interest rate, and σ is the volatility.

Consider the case when the underlying asset pays a continuous dividend [42] at some fixed rate q. Then, the Black Scholes equation becomes

$$\frac{\partial V}{\partial t} + \frac{1}{2}\sigma^2 S^2 \frac{\partial^2 V}{\partial S^2} + (r-q)S\frac{\partial V}{\partial S} - rV = 0. \tag{1.4}$$

When considering the case of an underlying asset of Forward or Future commodities [24], the Black Scholes equation becomes

$$\frac{\partial V}{\partial t} + \frac{1}{2}\sigma^2 F^2 \frac{\partial^2 V}{\partial F^2} - rV = 0. \tag{1.5}$$

where F denotes the Forward (Future) price.

In general, n-factor models [42] follow the equation

$$\frac{\partial V}{\partial t} + \frac{1}{2}\sum_{ij}^{n} \sigma_{ij}^2 S_i S_j \frac{\partial^2 V}{\partial S_i \partial S_j} + \sum_{i}^{n}(r-q_i)\frac{\partial V}{\partial S_i} - rV = 0, \tag{1.6}$$

where r is the risk free interest rate, q_i is the dividend yield of the i^{th} asset, t is time and $\sigma_{ij} = \sigma_i \rho_{ij} \sigma_j$ is the covariance of the i^{th} asset with respect to the j^{th} asset.

1.3 Literature Review of Option Valuation Methods

This section reviews existing option valuation methods.

1.3.1 Analytic and Approximation Solutions

Many option valuation problems can be solved for closed form solutions. Black and Scholes [1] obtained the closed form solutions for **European option**

$$C(S,t) = SN(d_1) - Ke^{-r(T-t)}N(d_2)$$

for the call option and

$$P(S,t) = Ke^{-r(T-t)}N(-d_2) - SN(-d_1)$$

for the put option. Above, the function $N(\cdot)$ is the standard normal distribution function, and

$$d_1 = \frac{\ln(\frac{S}{K}) + (r + \sigma^2/2)(T-t)}{\sigma\sqrt{T-t}} \tag{1.7}$$

$$d_2 = \frac{\ln(\frac{S}{K}) + (r - \sigma^2/2)(T-t)}{\sigma\sqrt{T-t}} \tag{1.8}$$

Analytic Solution of Barrier Options

Barrier options can also be solved in closed form. A typical barrier option is a down-and-out call option, which was first solved analytically by Merton in [29]. There has been extensive work on the pricing of double barrier options, or corridor options. Ikeda and Kuintomo (1992), and Geman and Yor (1996) have developed closed form solutions for double barrier options using quite complex mathematics. Haug [18] has developed an alternative way to value double barrier options using the single barrier put-call transformations in combination with some simple intuition. A closed-form formula for all types of continuous barrier options can be found in Haug [18]. It should be mentioned that in the market, most barrier options are monitored discretely, i.e., there is no closed form formula.

Analytic Approximation for American Options

It is possible to value perpetual **American options** in closed form [27]. There are quite a few analytical approximate solutions available. An early approach is the quadratic approximation of Barone-Adesi and Whaley [16]. Carr [8] introduced the randomization approach for pricing American options, and Huang et al. [21] introduced a recursive integral-equation method. It should be pointed out that all these analytical approximation methods still require a certain degree of computation.

To valuate the option price numerically, there are three methods, tree methods, Monte Carlo methods, finite difference methods.

1.3.2 Trees

The binomial tree method was suggested by Cox et al. [12], which approximates the underlying stochastic process as a lattice. Convergence of this method for **American** and path dependent options is proved in [26]. The binomial tree method using the fast Gauss transform is applied to American options in Broadie and Yamamoto [7].

Binomial methods converge slowly to the correct price for the case of **barrier options**. To overcome this, a trinomial tree approach is used by Boyle [3]. Figlewski and Gao [14] introduced an adaptive mesh method that increased the number of lattice nodes near the barrier. This greatly reduced the number of time steps required for accurate pricing.

1.3.3 Monte Carlo

Pricing financial options by Monte Carlo simulation is described in Boyle [2]. Broadie and Glasserman [18] obtained **American option** values by Monte Carlo simulation, with a high-low bias. Longstaff and Schwartz [28] proposed a Monte-Carlo method with a least-squares regression method, which is based on finding the value of the continuation function, or the expected future payoff, at each time step. Metwally and Atiya [30] made use of a Brownian bridge method for Monte Carlo simulation, which greatly increased the convergence rate.

In an attempt to reduce the complexity of pricing **path dependent options**, many have used variance reduction techniques to reduce computation time [34]. Monte Carlo simulation converges slowly but is usually easy to implement, and is still competitive for high dimensional problems, for which other methods cannot easily be applied.

1.3.4 Finite Differences

A partial differential equation framework for option pricing has faster convergence and has the advantage of providing the entire option value surface as well as the hedge factors, which can be useful for risk management.

The **Black-Scholes partial differential equation** can be transformed into a constant coefficient diffusion equation at which point the space discretization becomes easier [40]. The Black-Scholes equation also has time-dependence. First-order accurate explicit and implicit Euler schemes [40] are well-known methods for treating the temporal discretization. The implicit scheme is only first-order accurate, but it has good stability properties. The Crank-Nicolson method is second-order accurate in time, but it can produce undesired oscillations [44] to numerical solutions of Black-Scholes equation. One way to improve the stability is to use a Rannacher time-stepping scheme [33], which starts the time-stepping by a few implicit Euler time steps and then continues with the Crank-Nicolson method.

Finite Difference Methods for American Options

The pricing of an **American option** is a variational inequality problem [27]. Moreover, it can be formulated as a linear complementarity problem [37] [20]. Finite difference methods were suggested for use in finance by Brennan and Schwartz [5]. Jaillet et al. [25] proved the convergence of the Brennan and Schwartz method. The projected SOR method for pricing American options is introduced in [40]. Wu and Kwok [41] introduced front-fixing methods,

	Monte Carlo	Finite Difference	Trees
American/Bermudan	Not Great	Good	Good
Accuracy	Not Great	Good	Good
High dimensional Problems	Good	Not Great	Not Great

Table 1.1: Numerical Computational Techniques

Nielsen et al. [31] applied a nonlinear transformation to fix the boundary and solve the resulting nonlinear problem. Zvan et al. [43] introduced the penalty method and Nielsen et al. [32] further refined this model to a more general American type of option. Clarke and Parrott [10] applied multigrid methods to American options on assets with stochastic volatility.

Finite Differences Methods for Barrier Options

The discontinuities in exotic options such as **Barrier options** cause difficulties in obtaining numerical results, especially hedge parameters. Boyle and Tian [4] consider an explicit finite difference approach, which aligned grid points with barriers by constructing a grid which lies right of the barrier. Zvan et al. [45] introduced an implicit finite difference method for barrier options and the stability issues of discontinuous payoff. Tagliani [36] discussed discrete monitored barrier options by finite difference schemes. Vetzal et al. [39] discussed a general numerical approach of discrete Parisian and delayed barrier options.

In summary, one technique is not good for all problems. The three numerical techniques are summarized in Table 1.1.

1.4 Research Objectives

This research has two objectives. The first is to investigate adaptive mesh methods for exotic options such as barrier options. We want to improve existing methods for finding the price and Greeks of barrier options using an adaptive mesh method. The second is to investigate finite difference numerical methods of finding solutions for American options, and understand behaviors of the price and hedge factors of American barrier options.

1.5 Context

The rest of this project will be organized as follows. In Chapter 2, an adaptive mesh method is introduced and its application to Barrier options is presented in Chapter 3. The finite difference methods for valuating American options are investigated and behavior of hedge factors for American barrier options is further studied in Chapter 4. Chapter 5 summarizes the project.

Chapter 2

Adaptive Mesh Methods

In this chapter, we first describe a mechanism for generating non-uniform meshes based on the equidistribution principle in Section 2.1. Then the so-called moving mesh method is discussed in Section 2.2. In Section 2.3, a new adaptive mesh method is introduced.

2.1 Non-Uniform Mesh

The choice of an appropriate mesh is of high importance since it directly influences the numerical error. Basically, by choosing an appropriate non-uniform mesh, which locates more points in the regions that generate larger errors, it decreases the numerical error substantially. This is the core idea of the moving mesh strategy, where the number of grid points remains constant and only the locations of the grid points are changed with time.

2.1.1 Equidistribution Principle

De Boor's equidistribution principle (EP) has been a popular tool for mesh generation and adaptation [22]. The idea is to choose the coordinate transformation by equidistributing a monitor function, $M(x) > 0$, which provides some measure of the computational difficulty in the solution of the physical PDE. It can be expressed in its integral form [22] as

$$\int_0^{x(\xi,t)} M(\tilde{x},t)d\tilde{x} = \xi\theta(t),$$

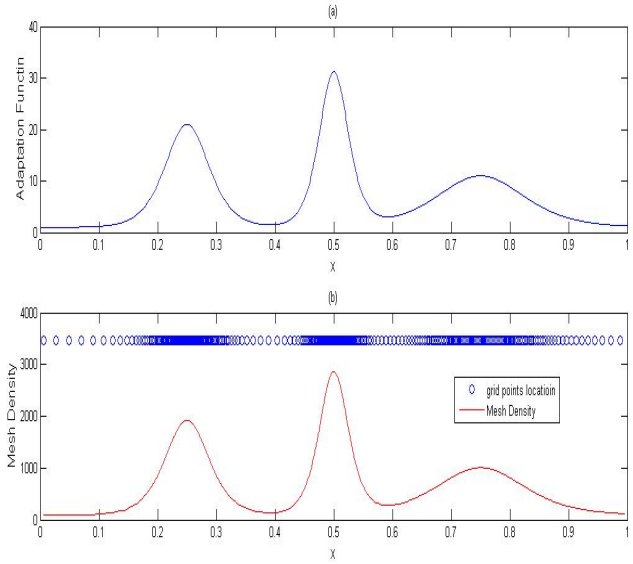

Figure 2.1: Mesh generator by De Boor's equidistribution principle

where

$$\theta(t) = \int_0^1 M(\tilde{x}, t)d\tilde{x}, \;\; \xi_i = \frac{i}{n}, \;\; i = 0, 1, ..., n.$$

In order to generate a mesh, one has to provide an adaptation function as shown in Figure 2.1(a). Figure 2.1(b) shows the location of the grid points and mesh density for the new mesh generated by the equidistribution principle.

2.2 Moving Mesh Method

For the numerical solution of time-dependent PDEs which involve large solution variations, a variety of moving mesh methods [23] have been shown to give significant improvements in accuracy and efficiency over conventional fixed mesh methods. When working properly (choosing a proper monitor function), a moving mesh method usually concentrates mesh points at regions of rapid variation in the solution. This produces commensurate accuracy and allows significantly larger time steps without causing instability [23]. Figure 2.2 (left) shows computed results using an adaptive moving mesh for Burgers' equation. Figure 2.2 (right) presents the mesh trajectories, which clearly show the concentration of grid points

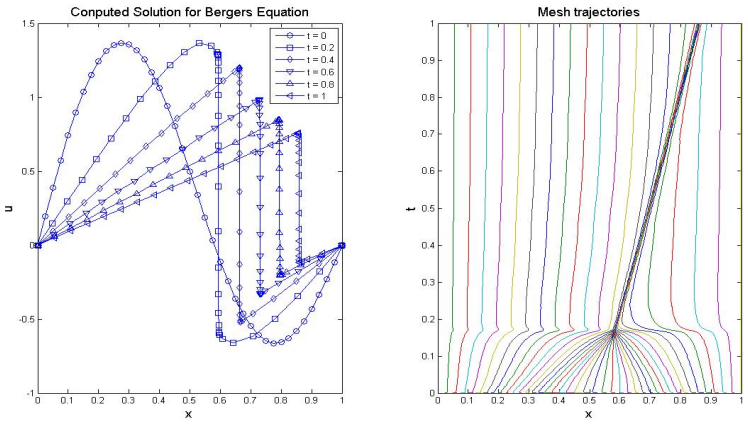

Figure 2.2: The graph of mesh adaptation of burger's equation using moving mesh solver.(a): The computed solution;(b): The corresponding mesh trajectories.

around the front.

2.2.1 Formulation of the Moving Mesh Method

Adaptive mesh movement is best understood by interpreting the problem in terms of a suitable coordinate transformation [22] $S = S(\xi, t)$ with

$$S: \ \Omega = [S_{min}, S_{max}] \rightarrow \Omega_c = [0, 1],$$

where Ω_c and Ω are the computational and physical domains, respectively. Generally speaking, this transformation is chosen such that the solution in the transformed spatial variable,

$$\hat{V}(\xi, t) = V(S(\xi, t), t),$$

is smooth and in principle economic to approximate using a uniform mesh on the computational domain Ω_c. A corresponding moving mesh can be described as

$$\mathrm{T}_h(t) : S_j(t) = S(\xi_j, t), \ \ j = 1, ..., N$$

which corresponds to a fixed, uniform mesh

$$\mathrm{T}_h^c(t) : \xi_j = \frac{j-1}{N-1}, \ \ = 1, ..., N$$

on Ω_c. A finite difference discretization of the Black-Scholes equation for $\hat{V}(\xi,t)$ on this moving mesh can be derived using the so-called *quasi-Lagrange approach*. The Black-Scholes equation is transfromed from the physical domain to the computational domain using the coordinate transformation shown below. By the chain rule,

$$\hat{V}_\xi = V_S S_\xi, \;\; \hat{V}_t = V_t + V_S S_t,$$

where $S_t = \frac{\partial S}{\partial t}(\xi,t)$ denotes the mesh speed. In the new coordinates (ξ,t), the Black-Scholes equation becomes

$$\hat{V}_t - \frac{\partial \hat{V}_\xi}{S_\xi} S_t = \frac{\sigma^2 S^2}{2}\left(\frac{\hat{V}_\xi}{S_\xi}\right)_\xi + (r-q)\frac{S}{S_\xi}\hat{V}_\xi + r\hat{V}. \tag{2.1}$$

2.2.2 Moving Mesh PDEs

The coordinate transformation $S = S(\xi,t)$ is determined by solving so-called moving mesh PDE (MMPDEs) [22]. Two popular choices are the

$$\begin{aligned} &MMPDE5 : \dot{x} = \frac{1}{\tau}\frac{\partial}{\partial\xi}(M\frac{\partial x}{\partial\xi}), \\ &MMPDE7 : \frac{\partial}{\partial\xi}(M\frac{\partial\dot{x}}{\partial\xi}) - 2\frac{\partial}{\partial\xi}(M\frac{\partial x}{\partial\xi})/\frac{\partial\dot{x}}{\partial\xi} = -\frac{1}{\tau}\frac{\partial}{\partial\xi}(M\frac{\partial x}{\partial\xi}), \end{aligned} \tag{2.2}$$

where $\dot{x} = \frac{\partial x}{\partial t}$, $\tau > 0$ is a parameter used for adjusting the time scale of the mesh movement, and the adaptation function $M(x,t) > 0$ provides some measure of the computational difficulty in the solution of the underlying physical differential equations. A popular choice for the adaptation function is

$$\rho = (1 + \frac{1}{\alpha}|u_{xx}|^2)^{\frac{1}{3}}, \tag{2.3}$$

where α is the intensity parameter given by

$$\alpha = \max\left\{1, \left[\int_0^1 |u_{xx}|^{\frac{2}{3}} dx\right]^3\right\}.$$

The discrete physical PDE and the meshing process form a coupled system. The system can be solved simultaneously and alternately. The simultaneous solution procedure has the advantage in one-dimensional problems, while for highly nonlinear and high dimensional problems, we usually resort to an alternate solution procedure.

2.3 New Adaptive Mesh Approach

Although the moving mesh method has done a great job in scientific computing, the moving mesh method takes extra CPU time to deal with MMPDEs, which will slow down the computational speed. By the property of Black-Scholes types of PDEs, the discontinuity or sharp front that arises in the modeling of option pricing usually only lasts for short time, and the singularity will smooth out quickly. In some cases of exotic options such as discrete barrier options, the discontinuity occurs frequently, but it still smooths out very fast in each interval between two monitor days. So using a pure moving mesh scheme will not provide as much computational efficiency benefit as in many other areas of scientific modeling.

2.3.1 Persson's Approach

Persson and Sydow [26] presented an adaptive technique to solve the Black-Scholes equation. The basic idea is to compute the solution on two coarse meshes (with $dx = 2h$ and $dx = h$), and then compute the difference $\tau = A_h u_h - A_{2h} u_{2h}$, where u_h and u_{2h} are the numerical solutions with initial grid $dx = 2h$ and $dx = h$, respectively, and A is the FD operator of Black-Scholes equation. Thereafter, the authors were able to construct a new non-uniform mesh using the mapping function

$$\hat{h}(x) = h(x) \left(\frac{\epsilon}{\epsilon\gamma + |\tau_h(x)|} \right)^{\frac{1}{p}},$$

which obtained a solution for the Black-Scholes equation which was twice as accurate as the solution using an equidistant grid with the same number of grid points.

2.3.2 New Approach

To balance the efficiency and accuracy, a new idea is to combine a moving mesh method and a non-uniform fixed mesh. This results in the following **algorithm**:

- Solve the problem once using a moving mesh method on a coarse grid, which automatically obtains information on the physical structure of the problem with time evolution. Give a measure π (adaptation function) to capture the numerical error distribution. At each time step, restore the value of the measure π on each grid point.

- Since the grid points are moving, interpolate the value of π at each time step to prefixed points. Then, take a time weighted average of these values to construct a mesh density distribution measure ρ.
- Create a new adaptive mesh based on the mesh density distribution.
- Solve the problem again with the new adaptive mesh using a fixed mesh solver.

Discretization of Black-Scholes Equation

The PDE is first discretiezed in the spatial domain, and then the resulting system of ordinary differential equations (ODEs) is integrated using an ODE solver (ode15i in Matlab). The main advantage of this method of lines is the separate treatments of the spatial and temporal components of the PDE, so that attention can be focussed on each of them independently.

The partial differential equation (2.1) can then be written as

$$\frac{\partial \hat{V}}{\partial t} = L\hat{V}. \tag{2.4}$$

where L is the FD-discretization operator.

For the spatial domain, central finite differences are used to discretize (2.1) on the uniform computational mesh T_h^c. This yields

$$\begin{aligned} L\hat{V} &= \frac{u_{j+1}-u_{j-1}}{S_{j+1}-S_{j-1}}\frac{dS_j}{dt} + \frac{\sigma^2 S_j^2}{S_{j+1}-S_{j-1}}\left[\frac{u_{j+1}-u_j}{S_{j+1}-S_j} - \frac{u_j-u_{j-1}}{S_j-S_{j-1}}\right] \\ &\quad +(r-q)S_j\frac{(u_{j+1}-u_{j-1})}{S_{j+1}-S_{j-1}} + ru_j. \text{ (for moving mesh)} \\ L\hat{V} &= \frac{\sigma^2 S_j^2}{S_{j+1}-S_{j-1}}\left[\frac{u_{j+1}-u_j}{S_{j+1}-S_j} - \frac{u_j-u_{j-1}}{S_j-S_{j-1}}\right] \\ &\quad + (r-q)S_j\frac{(u_{j+1}-u_{j-1})}{S_{j+1}-S_{j-1}} + ru_j. \text{ (for fixed mesh)} \end{aligned} \tag{2.5}$$

where $u_j(t) \approx \hat{V}(\xi_j, t) = u(S_j(t), t)$.

Time-integration and Time-adaptivity

For time-integration we use the backward difference formula of order two (BDF2) [19] . The time adaptive algorithm (ode15i in Matlab) chooses time-steps automatically to keep the local discretization error in time below or at a predefined level.

Chapter 3

Application to Barrier Options

In this chapter, we apply the adaptive mesh method to various barrier options and study some properties and hedge factors of barrier options.

The financial markets have invented **various types of barrier options**, such as an up-and-out barrier option, and a down-and-in barrier option. More complicated barrier options may have a time-dependent barrier, may have two barriers (double barrier options), and may have the final payoff determined by one asset and the barrier level determined by another asset (two-dimensional barrier options).

The **discontinuities** present in barrier options lends to difficulties in the numerical approximation of PDEs. Moreover, it can be shown that the sensitivities of the option price (the Greeks) satisfy the PDE with such discontinuous conditions involving Dirac functions [37].

3.1 Continuous Barrier Options

First, take the European double knock-out barrier call option with continuous monitoring barrier as an example. Let expiration date be T=3 months, strike price K=100, volatility $\sigma = 40\%$, interest rate r=10%, dividend rate q=2%, lower barrier $H_{lower} = 80$ and upper barrier $H_{upper} = 120$. If the underlying asset price goes above 120 or below 80 at any time before expiry, then the option is knocked out and the holder receives \$0. If the underlying asset price is always between \$80 and \$120, then the payoff is standard call option payoff $\max(S - K, 0)$.

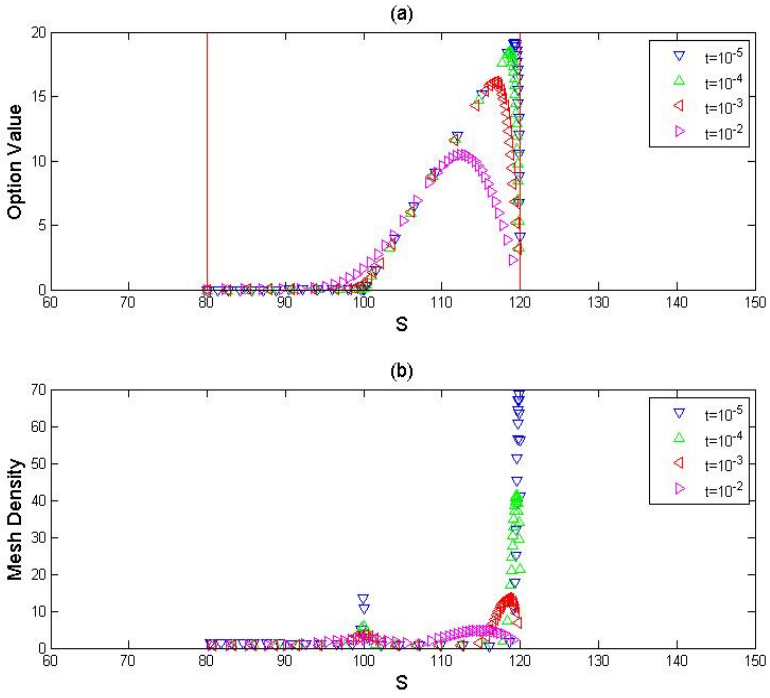

Figure 3.1: The graph of mesh adaptation at different times for the double knock-out continuous barrier option when using moving mesh solver

3.1.1 Moving Mesh Simulation

Take the function (2.3) as the adaptation function $M(x)$, and take MMPDE7 in equation (2.2) for the moving mesh solver. We compute this double knock-out barrier option with 81 grid points. Figure 3.1 (a) illustrates the mesh adaptation at different times. We can see that, initially, the solver automatically captures the steep slope area beside the upper barrier and the angle beside the strike price, and the grid points move and are concentrated in these two regions. Also when the physical solution smooths out, and the grid points become more evenly distributed. Figure 3.1 (b) further illustrates the mesh density change as the mesh moves.

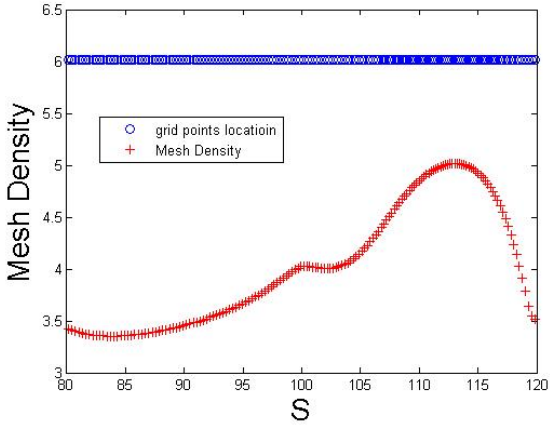

Figure 3.2: The graph of the new adaptive mesh for the double knock-out continuous barrier option.

3.1.2 Construct New Adaptive Mesh

At each time step of the moving mesh method, we restore the value of the adaptation function π on each grid point. Since the grid points are moving, we interpolate (using interp1.m in Matlab) the data to 81 pre-fixed equidistant points. Then, we take a time weight average of these values to construct ρ. Afterward, we use ρ as the mesh density distribution. Finally, based on this density measure ρ, we are able to generate a new adaptive mesh (see Figure 3.2). We construct a new mesh with 41, 81, 161, 321, 641, 1281 grid points within the domain of $S \in [80, 120]$, which have averages ΔS=1, 0.5, 0.25, 0.125, 0.0625, 0.0313, respectively.

3.1.3 Benchmark Analytical Solution

To study the numerical errors, we take the exact solution using Ikeda and Kuintomo's formula [18] with first five terms of their infinite series.

3.1.4 Accuracy Analysis

Figure 3.3 shows the results calculated on this new adaptive mesh with 1281 grid points, and average $\Delta S = 0.0313$. It shows that the numerical algorithm gives a very accurate result, with an error of $O(10^{-7})$. The numerical error between the equidistant mesh and

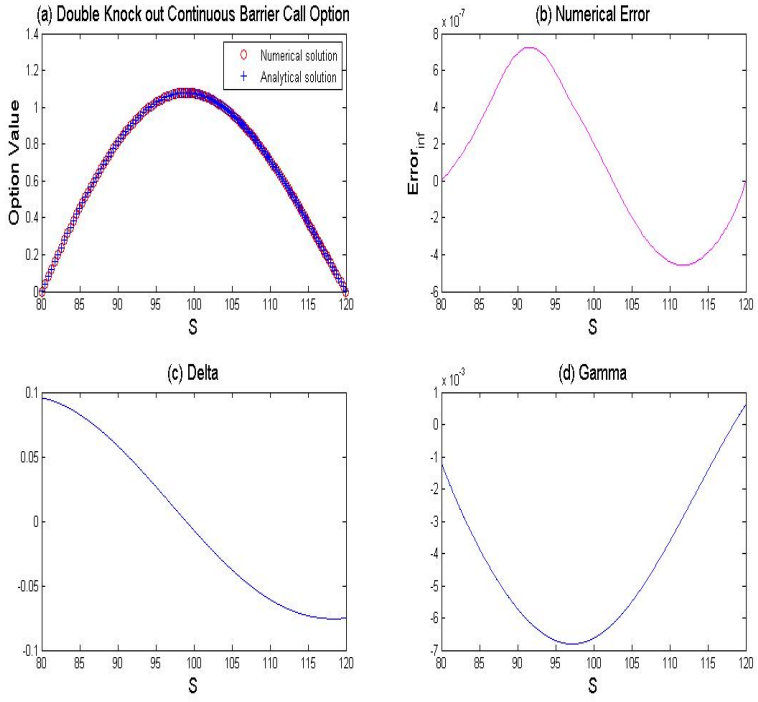

Figure 3.3: The graph of numerical results for the double knock-out continuous barrier option using an adaptive mesh method with 1281 grid points. (a) Numerical solution; (b) Numerical error compared to exact solution; (c) The Delta of the numerical solution; (d) The Gamma of the numerical solution.

ΔS	Equidistant Mesh	Adaptive Mesh
1	1.9824e-003	2.8560e-004
0.5	4.9531e-004	1.0724e-004
0.25	1.2395e-004	2.7400e-005
0.125	3.1075e-005	7.2559e-006
0.0625	7.8510e-006	2.6619e-006
0.03125	2.1196e-006	4.7179e-007

Table 3.1: Numerical errors for the continuous barrier call option using different meshes. Expiry date T=3 months, K=100, σ=40%, r=10%, q=2%, $H_{lower} = 80$, $H_{upper} = 120$. Both barriers are monitored continuously.

new adaptive mesh (ρ mesh) are studied in Table 3.1. The convergence study is also shown in Figure 3.4. From the table and the convergence log-log plot, we can see that the new mesh has substantially increased the accuracy.

3.2 Discrete Barrier Options

In this section, we study the discrete double knock-out barrier option. For discrete barrier options, discontinuity at the barrier occurs at each monitoring date, which brings more difficulty in obtaining an accurate result. The example considered here is a call option with expiration time of T=3 months, strike price K=100, volatility $\sigma = 40\%$, interest rate r=10%, dividend rate q=2%, lower barrier $H_{lower} = 80$, and upper barrier $H_{upper} = 120$. Then the barriers are monitored 10 times, i.e. at the $18^{th}, 36^{th}, 54^{th}, 72^{nd}, 90^{th}, 108^{th}, 126^{th}, 144^{th}, 162^{nd}, 180^{th}$ day.

3.2.1 Benchmark Solution

Since the exact option values are unknown, here we choose the result using the Quasi-Monte Carlo method, which simulates 80 million paths, as the exact solution.

3.2.2 Moving Mesh Simulation

Figure 3.5(a) shows how the moving mesh method reaches discontinuities of the barrier on a discrete barrier option. We can see that at the beginning, most grid points move and concentrate to the barrier region where there is a steep slope and sharp angle present. Once

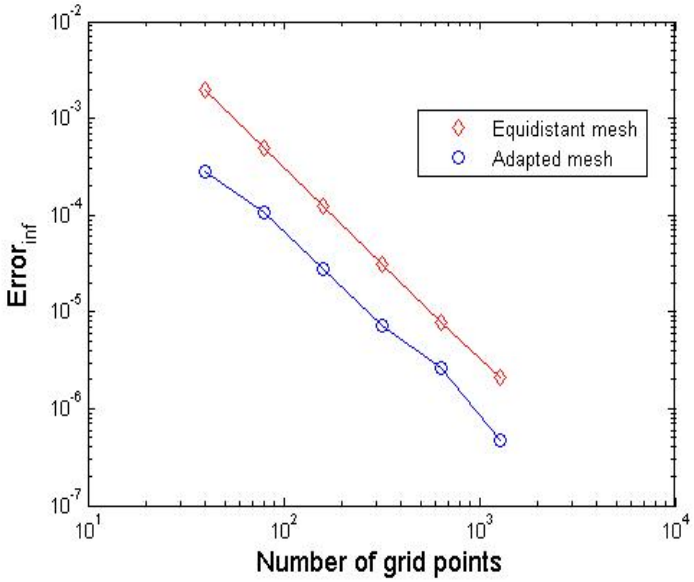

Figure 3.4: The log-log plot of the error convergence for the double knock-out continuous barrier option using different meshes.

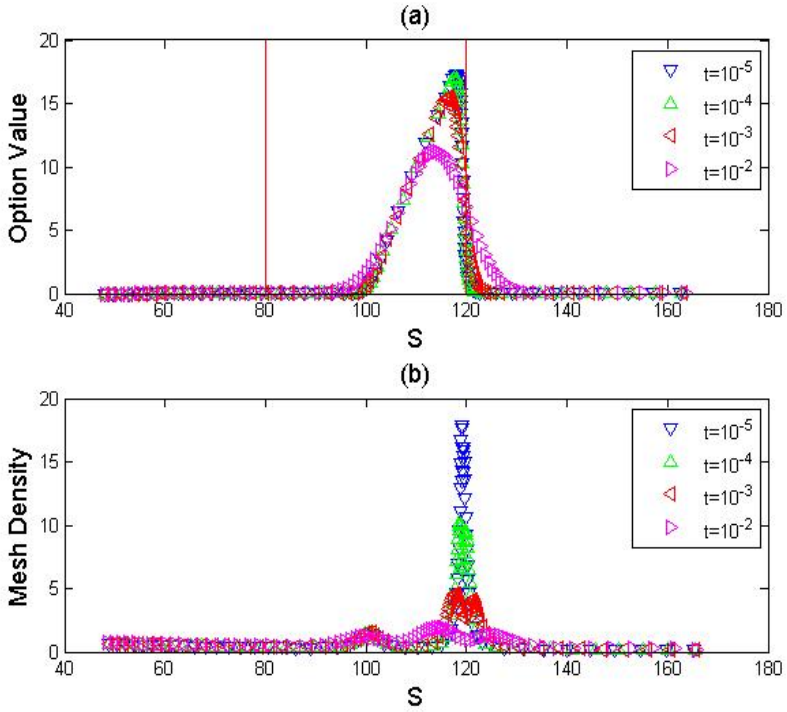

Figure 3.5: The graph of the mesh adaptation at different times for the discrete barrier option when using a moving mesh solver.

the solution of the barrier option smooths out, the grid points also smooth out and distribute more evenly. The mesh density in Figure 3.5(b) illustrates that the mesh density goes down as time passes.

3.2.3 Construct New Adaptive Mesh

After solving this model using a moving mesh solver, the density measure ρ is extracted. Then, we are able to generate a new adaptive mesh as in Figure 3.6. we construct new meshes with 41, 81, 161, 321, 641, 1281 grid points within the price range of $S \in [48, 168]$, and with average ΔS=3, 1.5, .75, 0.375, 0.1875, 0.0938, respectively.

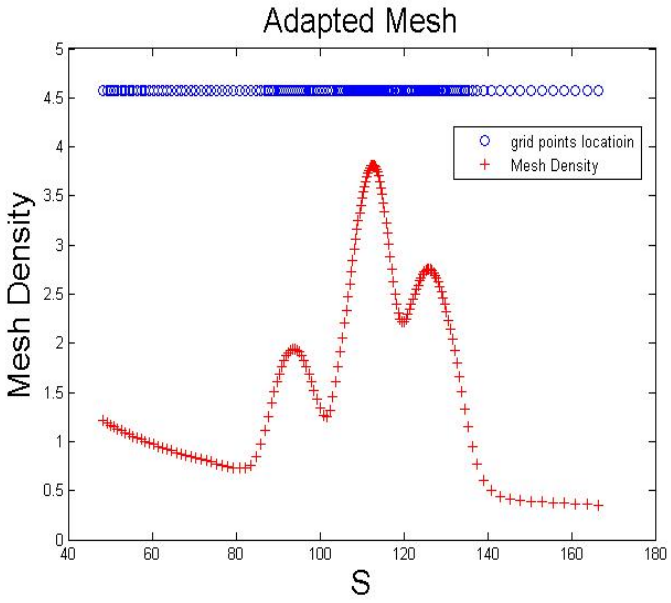

Figure 3.6: The graph of the new adaptive mesh for the discrete barrier option.

S	Monte Carlo	Equidistant Mesh	Adaptive Mesh	Moving Mesh
70	0.0103	0.0102	0.0101	0.0099
75	0.1022	0.1025	0.1019	0.1011
80	0.4060	0.4044	0.4047	0.4027
85	0.8730	0.8679	0.8722	0.8691
90	1.3245	1.3147	1.3245	1.3197
95	1.6515	1.6369	1.6522	1.6453
100	1.7998	1.7812	1.8009	1.7923
105	1.7403	1.7193	1.7419	1.7322
110	1.4779	1.4564	1.4797	1.4698
115	1.0700	1.0499	1.0709	1.0621
120	0.6336	0.6195	0.6352	0.6284
125	0.2985	0.2900	0.2991	0.2951
130	0.1101	0.1060	0.1101	0.1083

Table 3.2: Numerical solutions at asset price S for the discrete barrier call option using different meshes with 641 grid points. Expiry date T=3 months, K=100, σ=40%, r=10%, q=2%, $H_{lower} = 80$ and $H_{upper} = 120$. Both barriers are applied at the 10 monitor dates.

ΔS	Equidistant Mesh	Adaptive Mesh	Moving Mesh
3	0.2925	0.0242	0.0714
1.5	0.1602	0.0855	0.0373
0.75	0.0824	0.0334	0.0411
0.3750	0.0402	0.0076	0.0265
0.1875	0.0225	0.0022	0.0093

Table 3.3: Numerical errors for the double knock-out discrete barrier call option using different meshes. Expiry date T=3 months, K=100, σ=40%, r=10%, q=2%, $H_{lower} = 80$ and $H_{upper} = 120$. Both barriers are applied at 10 monitor dates.

3.2.4 Accuracy Analysis

With 641 grid points, the numerical solutions using a moving mesh, an adaptive mesh, an equidistant mesh and a Monte Carlo method are displayed in Table 3.2. The numerical errors using different meshes are shown in Table 3.3. As well, the point-wise errors are compared in Figure 3.7 and an error convergence log-log plot is presented in Figure 3.8. We can see that the new adaptive mesh obtains solutions with quadratic convergence, and the solutions are about five times more accurate than the results for an equidistant mesh. Furthermore, the new adaptive mesh method performs even better than the moving mesh method when using a large number of grid points, though it underperforms when the number of grid points is small.

3.3 Moving Barrier Options

A more challenging problem is the discrete and moving barrier case. Consider a double discrete moving barrier call option as an example. Let expiration time be T=3 months, strike price K=100, volatility $\sigma = 40\%$, interest rate r=10%, dividend rate q=2%, lower barrier $H_{lower} = 80$, and upper barrier $H_{upper} = 120$, where both barriers move outward one unit at each monitor day. Also, the barriers are monitored 10 times as in the previous plain discrete barrier case.

Again, we construct new adaptive meshes with 41, 81, 161, 321, 641 and 1281 grid points points separately (see Figure 3.9 for 161 points). The **benchmark solutions** are obtained by 80 million Quasi-Monte Carlo paths.

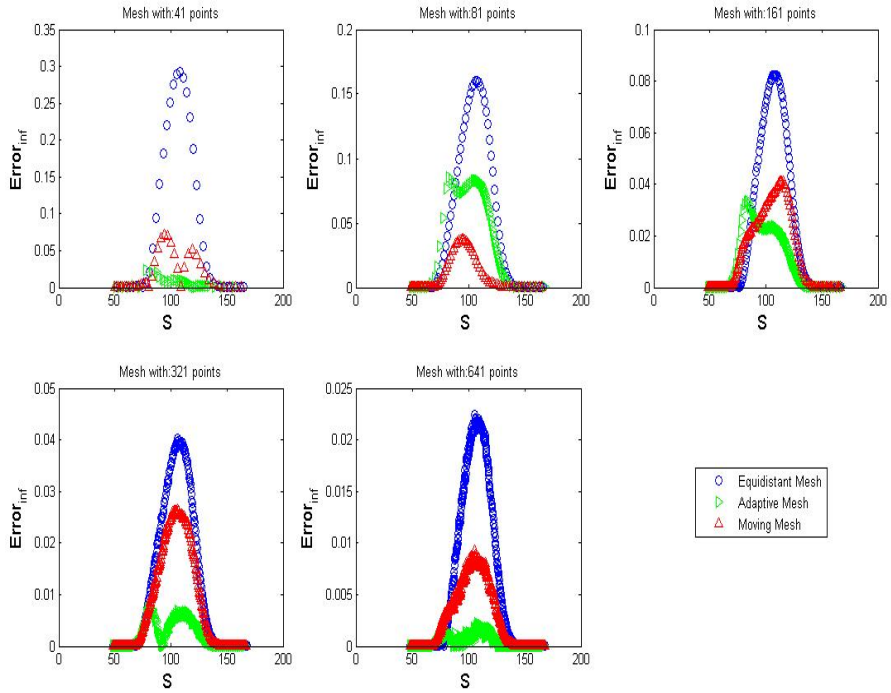

Figure 3.7: The graph comparing point-wise errors for the discrete barrier option using different meshes.

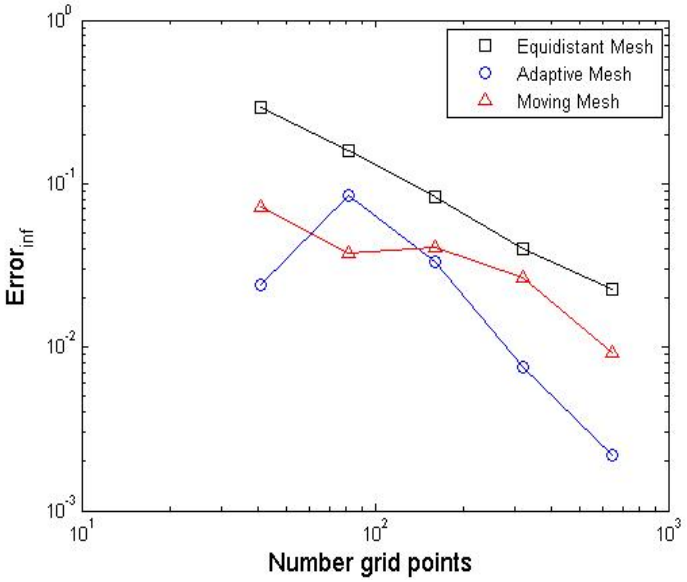

Figure 3.8: The log-log plot of the error convergence for the discrete barrier option using different meshes.

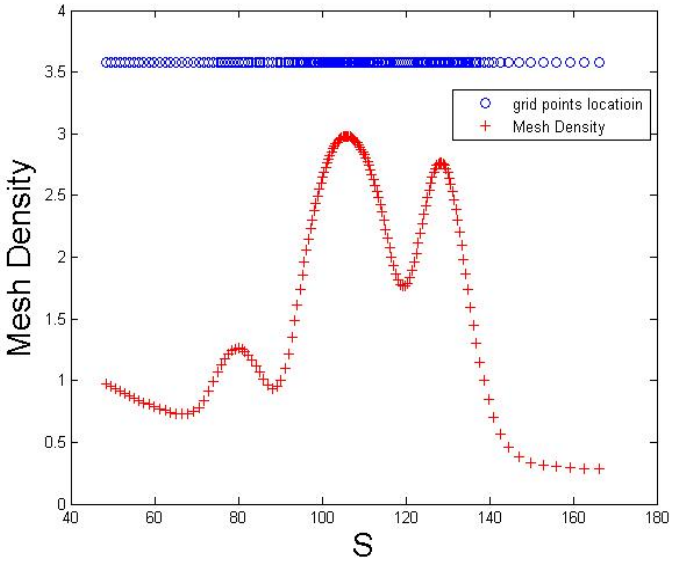

Figure 3.9: The graph of the new adaptive mesh for the moving discrete barrier option

S	Monte Carlo	Equidistant Mesh	Adaptive Mesh	Moving Mesh
70	0.1188	0.1181	0.1179	0.1179
75	0.3562	0.3546	0.3560	0.3546
80	0.7013	0.6982	0.7014	0.6982
85	1.1101	1.1058	1.1103	1.1059
90	1.5307	1.5228	1.5290	1.5231
95	1.8880	1.8785	1.8863	1.8791
100	2.1169	2.1058	2.1150	2.1070
105	2.1736	2.1609	2.1709	2.1626
110	2.0460	2.0332	2.0433	2.0354
115	1.7568	1.7442	1.7536	1.7469
120	1.3528	1.3413	1.3496	1.3450
125	0.9079	0.8989	0.9056	0.9035
130	0.5153	0.5084	0.5133	0.5131

Table 3.4: Numerical solutions at asset price S for the moving discrete barrier call option using different meshes with 641 grid points. Expiry date T=3 months, K=100, σ=40%, r=10%, q=2%, $H_{lower} = 80$ and $H_{upper} = 120$. Both barriers move outward one unit at each of the 10 monitor dates.

3.3.1 Accuracy Analysis

The numerical solutions with 641 grid points for these methods as well as Monte Carlo method are presented in Table 3.4. The infinity norm of the numerical errors on different meshes is shown in Table 3.5 and their point-wise numerical errors illustrated in Figure 3.10. We can see that the results with the new adaptive mesh are considerably better than the equidistant mesh, while the new adaptive ρ mesh even outperforms the moving mesh method, though it is better than the equidistant mesh. Figure 3.11 further illustrates the error convergence study for these three methods.

Remark: From the case of the discrete barrier and moving discrete barrier option, we noticed that the new adaptive mesh method outperforms the moving mesh method, and of course outperforms uniform mesh methods as well. It is speculated that this occurs because the barrier option smooths out after each monitor day. In the case of a moving mesh method, as time moves forward, grid moving will not increase the accuracy, but rather introduce additional error when doing the interpolation.

ΔS	Equidistant Mesh	Adaptive Mesh	Moving Mesh
3	0.1938	0.0318	0.0894
1.5	0.1099	0.0161	0.0740
0.75	0.0516	0.0101	0.0330
0.375	0.0279	0.0062	0.0143
0.1875	0.0137	0.0035	0.0117

Table 3.5: Numerical errors for the moving discrete barrier call option using different meshes. Expiry date T=3 months, K=100, σ=40%, r=10%, q=2%, $H_{lower} = 80$ and $H_{upper} = 120$. Both barriers move outward one unit at each of the 10 monitor dates.

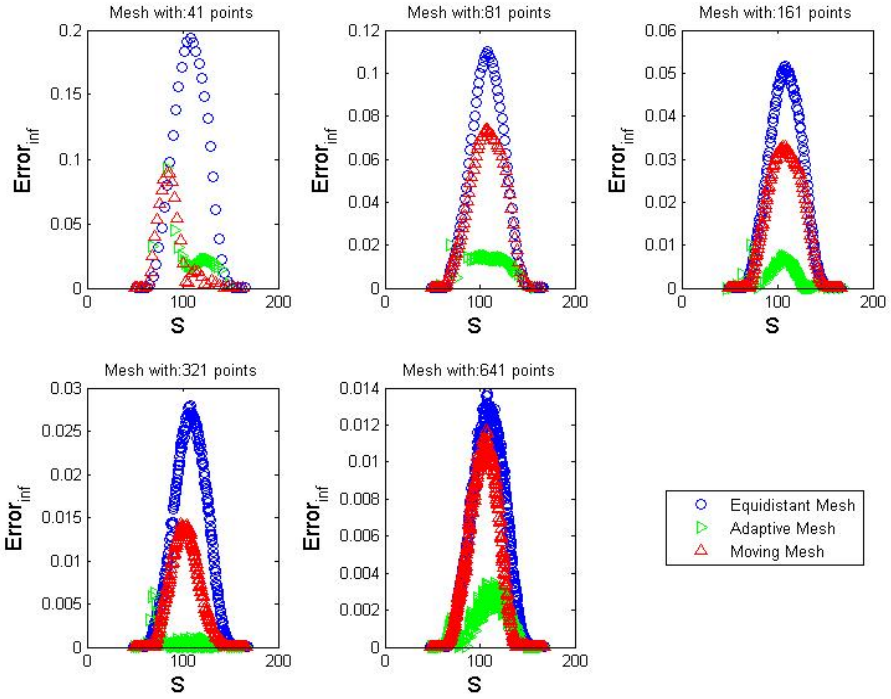

Figure 3.10: The graph comparing point-wise errors for the moving discrete barrier call option using different meshes.

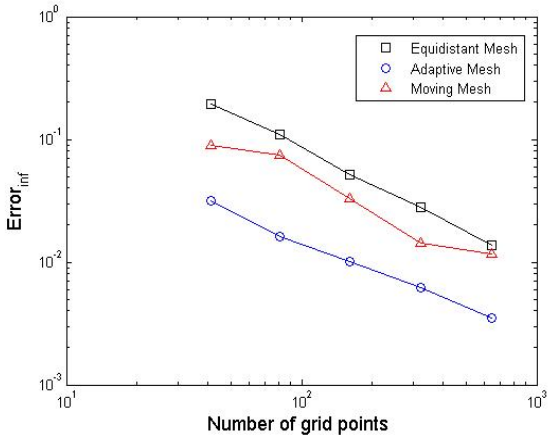

Figure 3.11: The log-log plot of the error convergence for the moving discrete barrier option using different meshes.

3.4 Further Study of Discrete Barrier Options

This section further studies the discrete barrier options, and mainly focuses on the influence of interest rate, dividend rate, volatility, monitoring frequency and hedge factors (Delta, Gamma, Vega, Rho). All the examples in this section are considering a double knock-out call option with expiry date T=3 months, strike price K=100, lower barrier $H_{lower} = 80$ and upper barrier $H_{upper} = 120$ with 30 monitoring days. The volatility, interest and dividend rates differ in each example.

3.4.1 Influence of the Dividend Rate on Discrete Barrier Options

Take a double knock-out call option with interest rate r= 10%, volatility $\sigma = 40\%$, and dividend rate q=2%, 6%, 10%, 14%, 18% separately. The results are presented in Figure 3.12. It is clear that as the dividend rate increases, the value of the option decreases. This matches the financial meaning, the payout dividend rate decreases the value of an option.

3.4.2 The Hedge Ratios of Discrete Barrier Options

This subsection focuses on the hedge factors (Delta, Gamma, Vega, Rho) of the discrete barrier options.

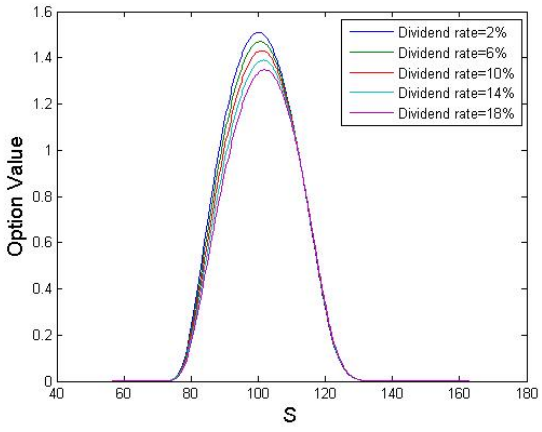

Figure 3.12: The graph of the influence of the dividend rate on the discrete barrier option.

The Delta factor is approximated by

$$\frac{\partial V}{\partial S} \approx \frac{V_{i+1} - V_{i-1}}{S_{j+1} - S_{j-1}}, \tag{3.1}$$

the Gamma factor is approximated by

$$\frac{\partial^2 V}{\partial S^2} \approx \frac{2}{S_{j+1} - S_{j-1}} \left[\frac{V_{j+1} - V_j}{S_{j+1} - S_j} - \frac{V_j - V_{j-1}}{S_j - S_{j-1}} \right], \tag{3.2}$$

the Rho factor is approximated by

$$\frac{\partial V}{\partial r} \approx \frac{V(r_{i+1}) - V(r_{i-1})}{2\Delta r}, \tag{3.3}$$

and the Vega factor is approximated by

$$\frac{\partial V}{\partial \sigma} \approx \frac{V(\sigma_{i+1}) - V(\sigma_{i-1})}{2\Delta \sigma}. \tag{3.4}$$

The Greek Delta

Take the case where the dividend rate q=2%, interest rate r=10%, volatility σ=40%, and consider when the option is close to maturity. Here we capture the Delta at times t=0.005, 0.001, 0.015, 0.02, 0.025 years, respectively. The results are shown in Figure 3.13. From the plot, we see that the option value becomes more and more sensitive as time approaches the expiry date. As well, the value of Delta is largest at the location of the upper barrier. When

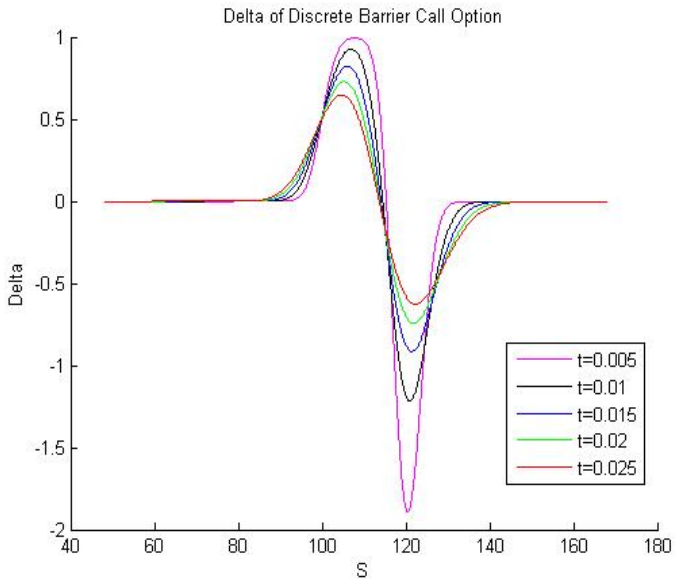

Figure 3.13: The graph of Delta for the discrete barrier option.

the underlying asset price is around the strike price, Delta is positive. However, when the asset price rises and is near the upper barrier, Delta becomes negative, due to the risk of hitting the barrier.

The Greek Gamma

Taking the same case considered in the previous example, we display Gamma at time t=0.005, 0.001, 0.015, 0.02, 0.025 years in Figure 3.14 (left). Figure 3.14 (right) gives a closer look at Gamma. It is apparent that when time is closer to the expiry date, Gamma is much higher, which means Delta is more sensitive. Moreover, Gamma gives a higher value when the asset price is close to strike price and a few units away from the upper barrier. Within the range from the strike price and the upper barrier, Gamma is almost negative, while outside this range, it is positive.

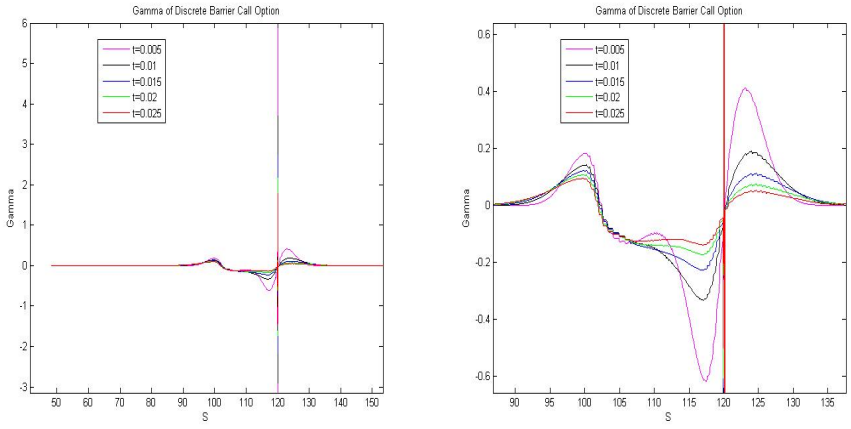

Figure 3.14: The graph of Gamma for the discrete barrier option.

Influence of the Interest Rate on Discrete Barrier Options and the Greek Rho

Figure 3.15 presents the results with fixed dividend rate q=5% and interest rate r=2%, 6%, 10%, 14%, 18%. Figure 3.16 further illustrates the Greek Rho for the discrete barrier option when interest rate r=6%, 10%, 14%. From the graph, we see that option value is positively correlated to the interest rate when it is out the money, but it is negatively correlated to the interest rate when it is in the money. This is due to the risk of hitting the barrier.

Influence of Volatility on Discrete Barrier Options and the Greek Vega

Consider a double knock-out call option with interest rate r=10%, dividend rate q=2% and volatility σ=10%, 20%, 30%, 40%, 50%, 60%. From Figure 3.17, we find that as the volatility increases, the value of the discrete barrier option decreases. This can be explained by the diffusion term $\frac{1}{2}\sigma^2 S^2 \frac{\partial^2 V}{\partial S^2}$ in the Black-Scholes equation. Since volatility is the coefficient of the diffusion term, increasing volatility will enlarge the effect of diffusion. Figure 3.18 shows the value of Vega for the discrete barrier option. In the case that the volatility is low, the option value is positively correlated to the volatility when the underlying asset price is less than the strike price. However, as the asset price goes up, Vega becomes negative since the option faces more risk of hitting the barrier. In the case that volatility is high, Vega almost becomes negative. This happens since the risk of hitting the barrier is high at high

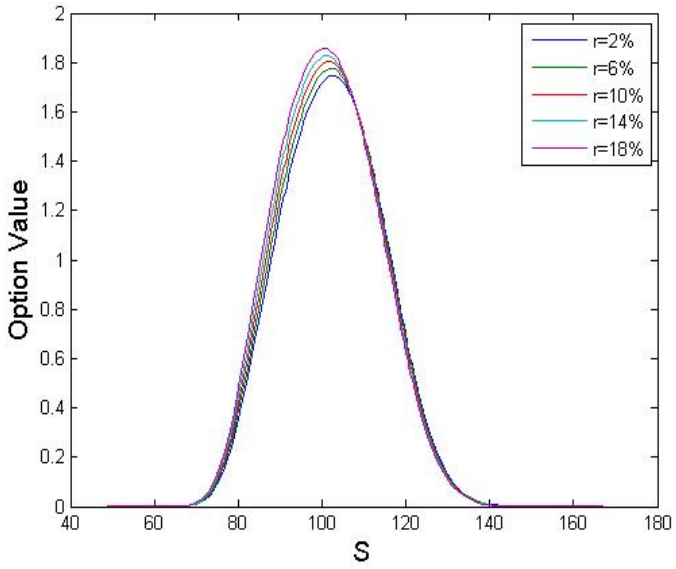

Figure 3.15: The graph of the influence of the interest rate on the discrete barrier option

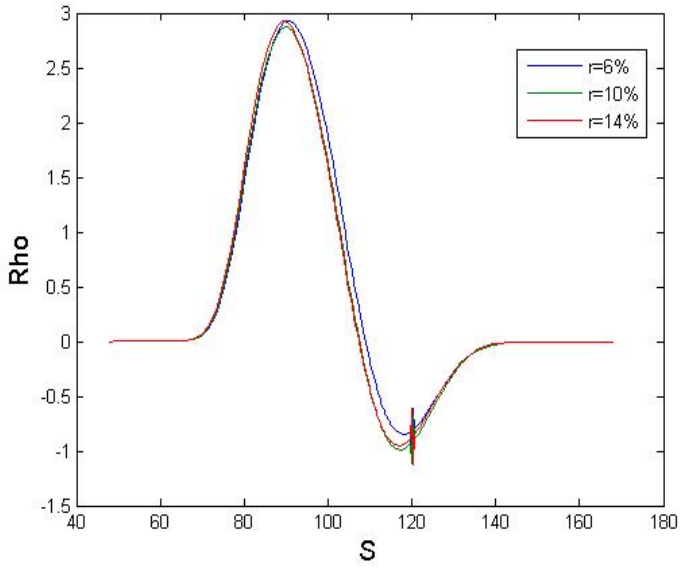

Figure 3.16: The graph of Rho for the discrete barrier option

levels of volatility.

3.4.3 Effect of Monitoring Frequency on Discrete Barrier Options

This subsection studies the effect of the monitor frequency on the value of the discrete barrier option.

Consider a double knock-out call option with expiry date T=3 months, strike price K=100, volatility $\sigma = 40\%$, interest rate r=10%, dividend rate q=2%, lower barrier $H_{lower} = 80$, upper barrier $H_{upper} = 120$, and discrete monitoring frequency of 10, 20, 40, 80, 160, 320 times. Figure 3.19 shows that the option value converges as the monitoring frequency rises.

Broadie et.al [6] proved that the price $V_m(H)$ of a discrete barrier option with m monitoring points can be approximated by a continuous barrier option $V(H)$ as

$$V_m(H) = V(He^{\pm\beta\sigma\sqrt{T/m}}) + o(1/\sqrt{m}), \tag{3.5}$$

with + for an up barrier option and - for a down barrier option. Above, the constant β is

$$\beta = -(\zeta(1/2)/\sqrt{2\pi}) \approx 0.5826,$$

where ζ is the Riemann zeta function.

Table 3.6 illustrates the numerical difference between the discrete barrier option value and the continuous barrier option with barrier shifted by $\exp(\beta\sigma\sqrt{T/m})$. The difference seems to decrease linearly in $\frac{1}{\sqrt{m}}$. The higher ratio for cases with m=320 and 640 times can be explained by the numerical error that was caused by too many discontinuities in cases of high monitoring frequency. The log-log plot in Figure 3.20 provides further support for the linearity.

3.5 Conclusions

An adaptive mesh method has been developed for efficiently dealing with the Black-Scholes equation for various types of barrier options. The adaptive meshes are chosen such that the mesh nodes are relocated in the regions which involve large numerical errors, which will reduce the final global error substantially. The algorithm automatically selects the grid by using a moving mesh solver, which runs in a coarse mesh and obtains the structure of

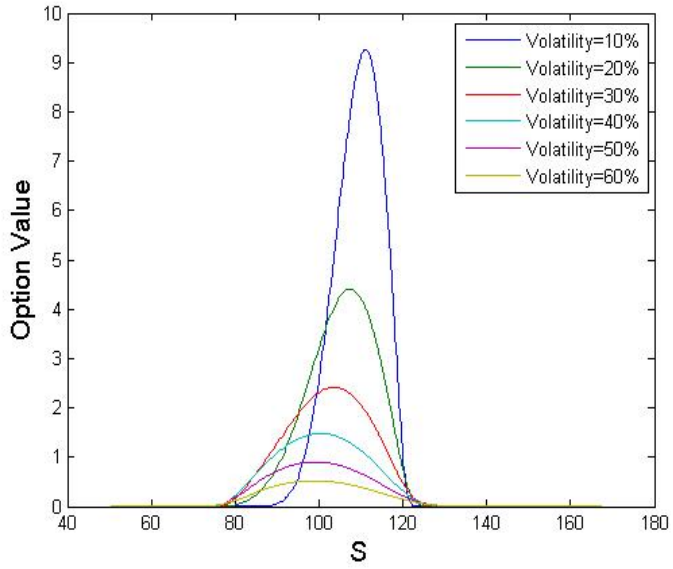

Figure 3.17: The graph of the influence of the volatility on the discrete barrier option.

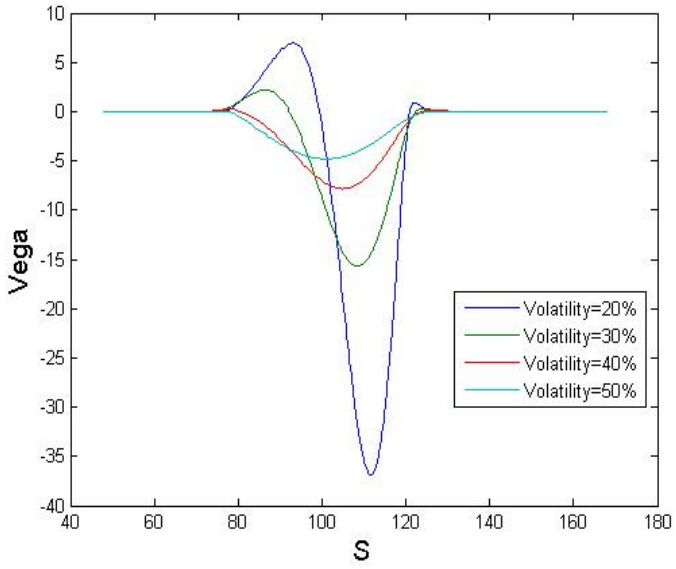

Figure 3.18: The graph of Vega for the discrete barrier option.

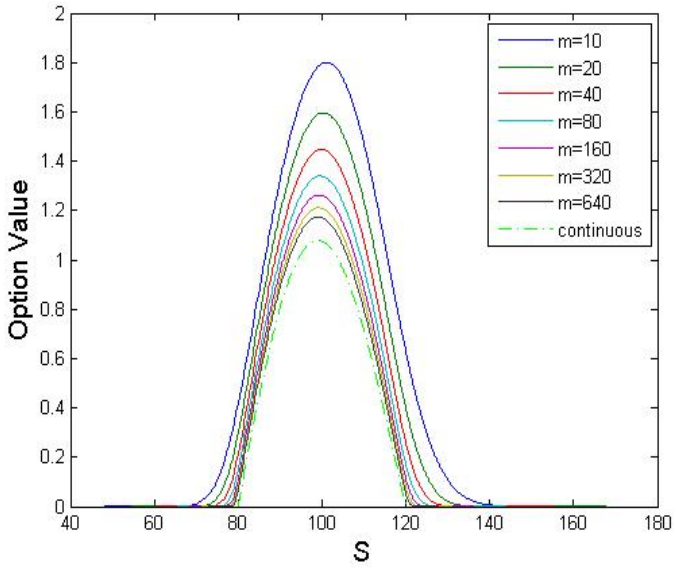

Figure 3.19: The graph comparing continuous barrier options with discrete barrier options.

m	Error	$\frac{1}{\sqrt{m}}$	Ratio
10	0.4145	0.3162	1.3107
20	0.2954	0.2236	1.3211
40	0.2090	0.1581	1.3221
80	0.1490	0.1118	1.3325
160	0.1080	0.0791	1.3662
320	0.0807	0.0559	1.4432
640	0.0673	0.0395	1.7025

Table 3.6: Discrete barrier option monitoring frequency convergence. T=3 months, K=100, σ=40%, r=10%, q=2%, $H_{lower} = 80$ and $H_{upper} = 120$. The barriers are monitored discretely with frequency m=10, 20, 40, 80, 160, 320 times, respectively; the 'Error' is the difference of the value of discrete barrier and it's continuous modification (3.5); the 'Ratio' is the ratio of 'Error' and '$\frac{1}{\sqrt{m}}$'.

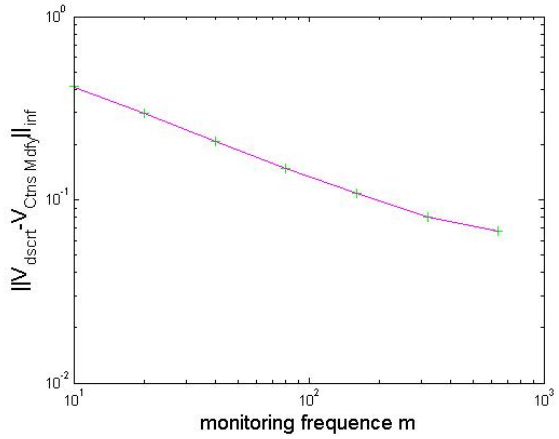

Figure 3.20: The log-log plot of the convergence of discrete barrier options to continuous barrier option versus the monitoring frequency m.

the solution for an option model. The method has been tested successfully for problems with three different types of barrier option. The moving mesh method performs best when using few grid points, since it automatically moves the grid points to the right locations at each time step, which reduces the numerical error. However, as the number of grid points increase, it does not have this advantage, since the singularity smooths out as time evolves. The adaptive mesh method combines the merit of moving mesh method and the efficiency of fixed mesh methods. It is able to obtain more accurate solutions without taking much additional computational time. In order to give insight into hedging discrete barrier options, we did several numerical simulations to further study the hedge factors for discrete barrier options.

Chapter 4

American Options

This chapter investigates several finite difference numerical methods for valuating American options in both one-dimension and two dimension cases. Then, the price behavior and hedge factors of American barrier options with continuous and discrete barriers are further studied.

4.1 Formulation of American Option Models

An American style derivative is a contract whose cash flows can be influenced by the holder of the derivative. The holder affects the cash flows of the contract through an exercise strategy. The optimal exercise strategy is the one which will provide the holder of the option with the maximum value.

The pricing of American options is a similar physical phenomenon to the obstacle problem. The obstacle problem arises when an elastic string, which is fixed at two ends A and B, passes over a smooth object which protrudes between the two ends (Figure 4.1).

Similarly, for American put options, the obstacle is the payoff function $\max(K - S, 0)$. The pricing of American options can be formed into a linear complementarity problem. For

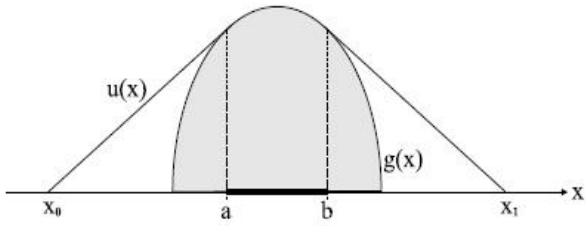

Figure 4.1: Obstacle Problem.

example, an American put option can be formularized [40] [20] by the following equation:

$$\begin{aligned}
\text{for } S < S_f(t): \quad & V(S,t) = K - S \qquad \textit{and} \\
& \tfrac{\partial V}{\partial t} + \tfrac{1}{2}\sigma^2 S^2 \tfrac{\partial^2 V}{\partial S^2} + (r-q)S\tfrac{\partial V}{\partial S} - rV < 0, \\
\text{for } S > S_f(t): \quad & V(S,t) > K - S \qquad \textit{and} \\
& \tfrac{\partial V}{\partial t} + \tfrac{1}{2}\sigma^2 S^2 \tfrac{\partial^2 V}{\partial S^2} + (r-q)S\tfrac{\partial V}{\partial S} - rV = 0 \\
\text{boundary condition:} \quad & \lim_{S\to\infty} V(S,t) = 0 \\
& V(S_f(t),t) = K - S_f(t) \\
& V_S(S_f(t),t) = -1 \\
\text{initial condition:} \quad & V(S,T) = \max(K-S,0)
\end{aligned}$$

where V is the option value, K is the strike price, S is the underlying asset price and $S_f(t)$ is the optimal exercise boundary.

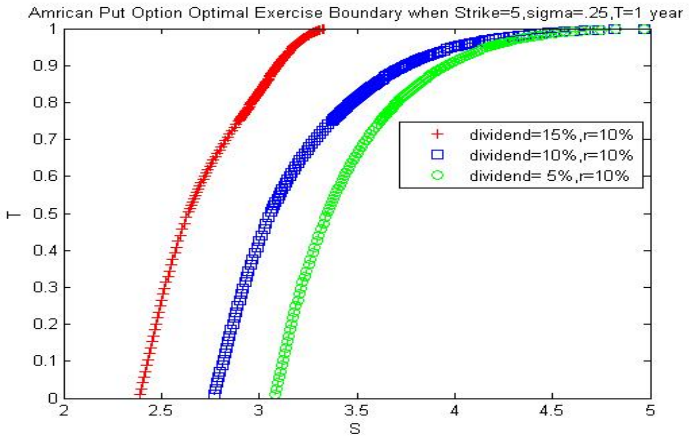

Figure 4.2: The graph of optimal exercise boundary for American put options in case of $r > q$, $r = q$, $r < q$.

4.2 Optimal Exercise Boundary

The free boundaries (optimal exercise boundary) $S_f(t)$ relates to the optimal exercise strategy, which will provide the holder of the option with the maximum value. The free boundary separates the region where it is optimal to exercise the option from the region and where it is optimal to hold the option.

Although closed form solutions for the American option optimal exercise boundary do not exist, several analytical approximations near expiry have been derived. Kuske et al. [13] derived an analytical approximation of the optimal exercise boundary near expiry. Recently, a iterative numerical algorithm has been introduced by several authors (Coman [11]), which is based on using an initial free boundary approximation and then doing several iterations with the transformed Black-Scholes equation. The sequence of boundaries converge monotonically to the optimal exercise boundary. Figure 4.2 illustrates the optimal exercise boundary obtained by Coman's iterative algorithm.

4.3 Numerical Schemes for Valuating American Options

In this section, we discuss finite difference schemes for valuating American options. Numerical experiments are provided to illustrate the convergence behavior and runtime speed of

these methods.

4.3.1 The Schemes

The finite difference numerical methods studied in this section are the Brennan Schwartz scheme [5], the projected successive over-relaxation algorithm [40], the penalty scheme introduced by Zvan et al. [43] and explicit front fixing method introduced by H. Han and X. Wu [17].

4.3.2 Comparison of Finite Difference Schemes

This subsection studies the convergence behavior providing insight into the FD methods as presented. We consider an American put option with expiry date T=2 years, strike price K=5, volatility σ=25%, interest rate r=10% and dividend rate q=15%. All the algorithms are implemented using MATLAB for testing purposes, and the computations are carried out on a 4×1.1 Ghz SunFire V440 machine with 8 GB of RAM. For all these schemes we did the numerical experiments with 21, 41, 81, 161, 321, 641, 1281 equidistant grid points within domain $S \in [0.6767, 20]$.

Benchmark Solution

Since the exact option values are unknown, we use the binomial method with large steps (80000) to find the option values. The results of the binomial method with large steps are considered very accurate. Thus we take these values as the exact option values for the purpose of comparison.

Accuracy Analysis

Table 4.1 lists the numerical solutions using a mesh with 641 grid points. The solutions using the binomial tree method are also displayed for comparison. Table 4.2 shows the numerical errors and its log-log plot is further illustrated in Figure 4.3. We notice that all these finite different schemes are very accurate, since they obtain an error of $O(10^{-4})$ with only 81 grid points. We also notice that the penalty scheme out performs other schemes and has a quadratical convergence rate, which matches the quadratical convergence conclusion in [15]. The PSOR method converges similarly to the penalty method, though its error is

S	$BinTree$	$PSOR$	BS	$PNLTY$	$FRONT$
2	3	3	3	3	3
3	2.0525	2.0525	2.0525	2.0525	2.0525
4	1.3297	1.3297	1.3296	1.3297	1.3296
5	0.82151	0.82151	0.82151	0.82151	0.82149
6	0.49101	0.491	0.491	0.49101	0.491
7	0.28779	0.28778	0.28779	0.28779	0.28779
8	0.16709	0.16708	0.16709	0.16709	0.16709
9	0.096769	0.096754	0.096772	0.096772	0.096771
10	0.056161	0.056137	0.056163	0.056163	0.056162

Table 4.1: Numerical solutions for finite difference schemes and binomial tree method for American put option with T=2 years, K=5, σ=25%, r=10% and dividend rate=15%. 'BinTree' denotes binomial tree method, 'PSOR' denotes projected successive over-relaxation algorithm, 'BS' denotes Brennan Schwartz scheme, 'PNLTY' denotes penalty scheme, 'FRONT' denotes explicit front tracking scheme. The results were computed on a equidistant mesh with 641 grid points.

ΔS	$PSOR$	BS	$PNLTY$	$FRONT$
1	1.0401e-002	1.0400e-002	1.0401e-002	1.0400e-002
0.5	4.7861e-003	4.8158e-003	4.7860e-003	4.8158e-003
0.25	6.5912e-004	6.6478e-004	6.5894e-004	6.6478e-004
0.125	1.4875e-004	1.8870e-004	1.4875e-004	1.8870e-004
0.0625	6.9414e-005	1.1979e-004	6.9412e-005	1.1979e-004
0.03125	3.7202e-005	5.7175e-005	3.7202e-005	5.7560e-005
0.015625	2.4651e-005	5.6157e-005	1.9902e-005	5.6157e-005

Table 4.2: Numerical errors for finite difference schemes compared to binomial tree method using equidistant meshes with 21, 41, 81, 161, 321, 641, 1281 grid points, respectively.

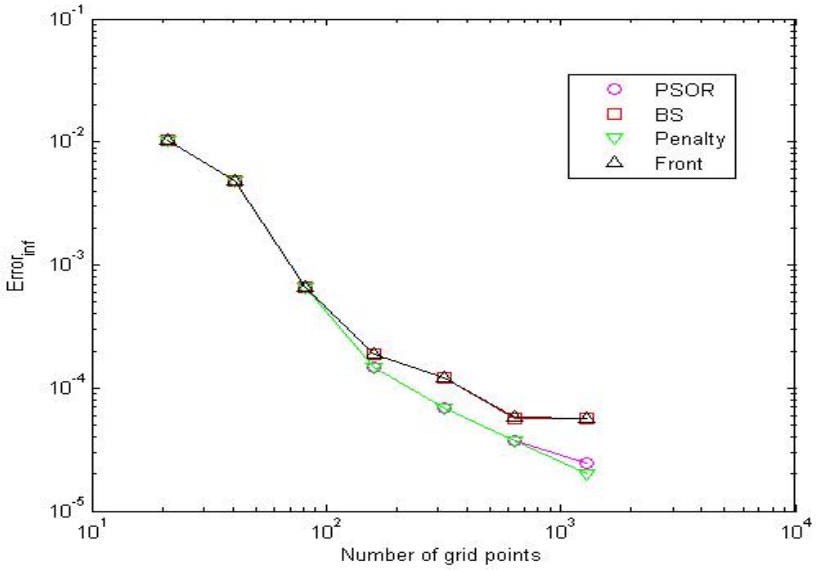

Figure 4.3: The log-log plot of numerical error convergence for the American put option using different finite difference schemes.

Grid Points	SOR	BS	$PNLTY$	$FRONT$
21	3.751	1.8967	3.8709	2.0616
41	13.274	6.4778	17.38	6.0646
81	30.315	17.699	35.868	15.732
161	62.63	34.083	77.072	34.875
321	124.67	81.013	217.15	56.286
641	1293.5	172.43	598.89	186.9
1281	4960.8	527.41	1740.1	526.93

Table 4.3: CPU time (in seconds) used for finite difference schemes for solving the one dimensional American put option.

a little bit higher when the number of grid points is large. The Brennan Schwartz scheme and the explicit front tracking scheme perform quite similarly, but they both have much higher error than the penalty scheme. The numerical error for these two schemes also tends to converge slower as the grid points increase.

Runtime Comparisons

The CPU time of each of these schemes are shown in Table 4.3 with its log-log plot illustrated in Figure 4.4. We find that the explicit front tracking scheme is a little bit faster than the Brennan Schwartz scheme, and they are both much faster than the other two schemes. The runtime of the penalty scheme increases similarly compared to the Brannan Schwartz scheme, as the number of grid points increases, though it takes more time computing. The PSOR scheme is not so slow when using fewer grid points, but slows down substantially when the number of grid points are increased.

Two Dimensional Case

In order to give further insight into the runtime speed of these finite difference schemes, we consider a two asset American basket option with expiry date T=1 year, strike price K=20, interest rate r=10%, asset S_1 with volatility σ_1=40%, dividend rate q_1=3%, asset S_2 with volatility σ_2=40%, dividend rate q_2=3% and correlation $\rho(S_1, S_2) = -0.7$. The resulting Black-Scholes equation has the form as in equation (1.5). The initial value is taken as $V_0 = \max(\max(S_1, S_2) - K, 0)$. The space domain is $(S_1, S_2) \in [1, 40] \times [1, 40]$.

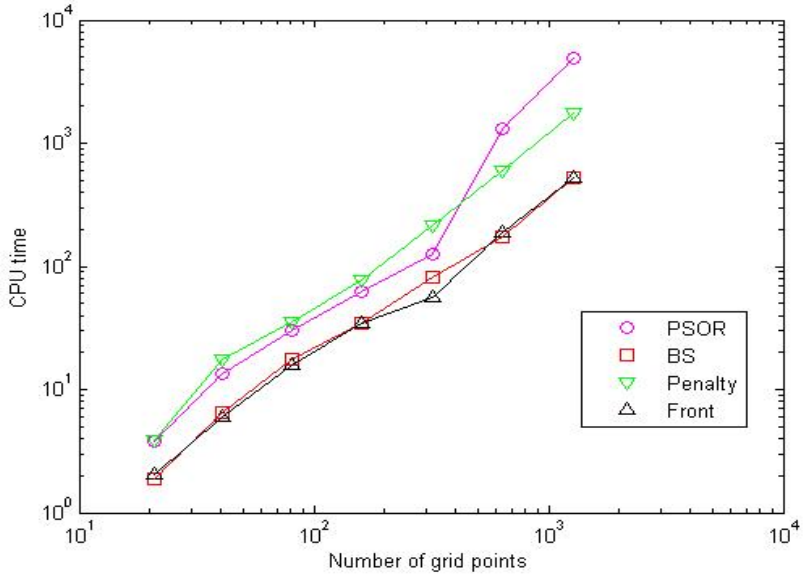

Figure 4.4: The log-log plot of runtime comparisons for the American put option using different finite difference schemes.

Since the explicit front tracking scheme can only be applied in the one dimensional case, we compare the PSOR scheme, the Brennan Schwartz scheme and the penalty scheme. The penalty scheme is combined with the large linear system solver conjugate gradients squared method (CGS) [35] and biconjugate gradients stabilized method (BiCGstab) [38]. The CPU time expense of each of these schemes is presented in Table 4.4.

We notice that as the number of grid points increases, the CPU time used by the Brennan Schwartz scheme substantially grows. The CPU time used by the PSOR scheme does not grows as fast as the Brennan Schwartz scheme, but it is much larger than that of the penalty scheme with BiCGstab and CGS. We also noticed that the CGS scheme performs a little bit better than the BiCGstab scheme.

Remark:

For solving one dimensional American option models, when using a small number of grid points, the Brennan Schwartz scheme and the explicit front tracking scheme are better candidates which spend less CPU time. However, when we require higher accuracy, i.e.,

Grid Points	BiCGstab	CGS	PSOR	BS
11×11	20.564	15.327	9.0695	7.4644
21×21	17.983	14.545	37.863	88.547
41×41	26.907	19.582	147.7	2154.5
81×81	108.76	91.323	854.05	77798

Table 4.4: CPU time (in seconds) used for finite difference schemes for solving the two dimensional American option. 'BiCGstab' denotes penalty scheme with BiCGstab solver, 'CGS' denotes penalty scheme with CGS solver, 'PSOR' denotes projected successive over-relaxation algorithm, 'BS' denotes Brennan Schwartz scheme.

more grid points, the penalty would be a good choice. For solving higher dimensional American option models, the penalty methods seemed to be more flexible and efficient, where the modern large sparse algebraic solvers, such as BiCGstab or CGS, can be applied. Although the Brennan Schwartz scheme performs well in the one-dimensional case, it is not a good choice in higher dimensional models.

4.4 American Barrier Option

In this section, we study the American barrier options. We mainly focus on the influence of a continuous monitoring barrier and a discrete monitoring barrier on option value and hedge factors (Delta, Gamma, Vega, Rho) for American barrier options.

4.4.1 Numerical Scheme

All the numerical results are computed using the penalty scheme [43]. Since we have not been able to apply the adaptive mesh method to American option, in order to concentrate more points around the barrier and strike price, we use the following function as the mesh density distribution measure:

$$\rho = 1 + 3(1 - \tanh(40(S - K))^2) + 6(1 - \tanh(40(S - H))^2),$$

where K is the strike price, H is the barrier. The resulting non-uniform mesh is shown in Fig 4.5. For the time-integration we use BDF2 [19].

For computing the hedge factors we use the same formula as in equations 3.1 $\sim$ 3.4.

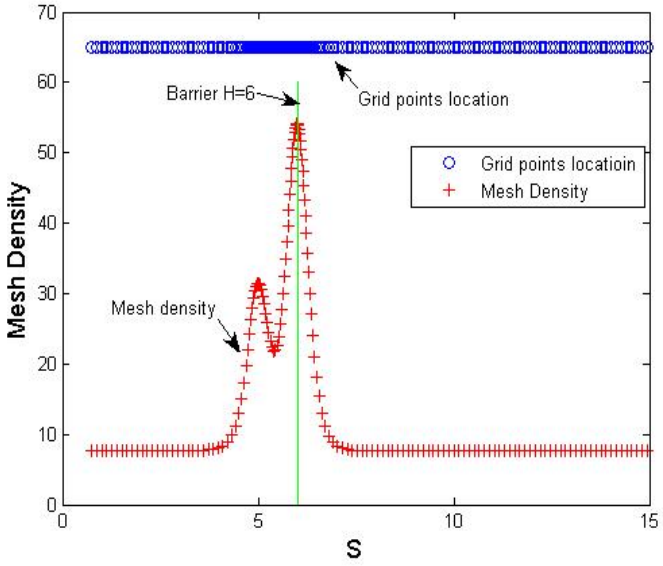

Figure 4.5: The graph of the non-uniform mesh for the American put barrier option.

All the examples in this section are computed on a non-uniform mesh with 641 grid points and consider an American up-and-out barrier put option with expiry date T=2 years, strike price=5 and dividend rate=15%. The volatility, interest rate and knock out barrier change from case to case.

4.4.2 American Option Value with and without Barriers

We take volatility=40%, interest rate=10% and knock out barrier H=6. Figure 4.6 illustrates the numerical solutions for a regular American put option, a continuous monitored American put barrier option, and a discrete monitored American put barrier option. From the graph we find that the option value of the regular American put option is greater than the ones with discrete barriers. As well, the put with a discrete barrier is greater than that with discontinuous barriers. Figure 4.7 further shows the value of Delta for these three options. We find that the price of the continuous barrier put option is the least sensitive and that the value of Delta for the discrete barrier put option is smaller than that of a regular American put when the underlying asset price is small, while it is greater when the option is deep in the money.

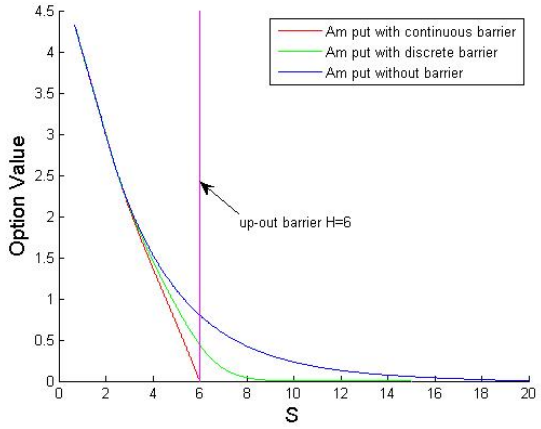

Figure 4.6: The value of the American barrier put option.

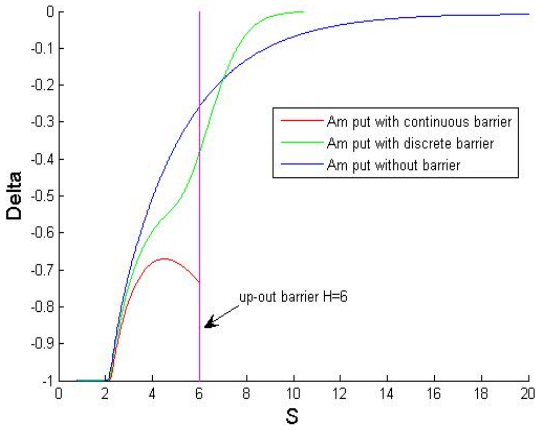

Figure 4.7: The value of Delta of the American barrier put option.

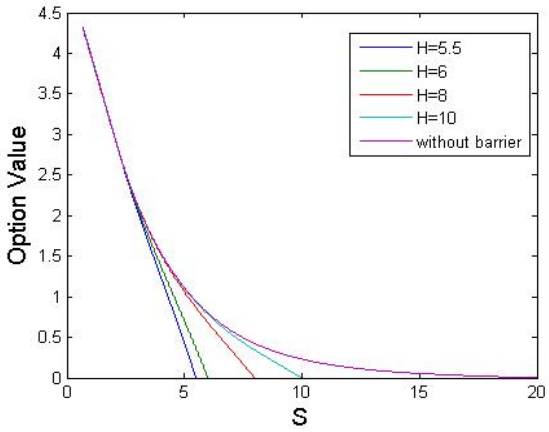

Figure 4.8: The influence of the barrier on the American put option price. The barriers are continuously monitored, where H=[5.5, 6, 8, 10].

4.4.3 Influence of Barrier on the American Option Value, Delta and Gamma

This subsection studies the influence of the barrier on the price and hedge factors Delta and Gamma of American options.

Continuous Barrier Case

Firstly, consider an American put option with continuously monitored knock-out barrier H at 5.5, 6, 8, 10 separately. Figure 4.8 presents the numerical results with these different barriers. We find that as the barrier moves outward, the value of the American option also increases and the option value becomes closer to a regular American put option with the same parameters.

Discrete Barrier Case

Consider an American put option with discretely monitored knock-out barrier H which takes values 5.5, 6, 8, 10 separately. These barriers are monitored at 10 discrete times. Figure 4.9 displays numerical solutions for these options. Figure 4.10 and Figure 4.11 further illustrate the influence of monitoring barrier on the value of Delta and Gamma for American discrete barrier options. We notice that Delta is twisted when the barrier is closed to strike price. As

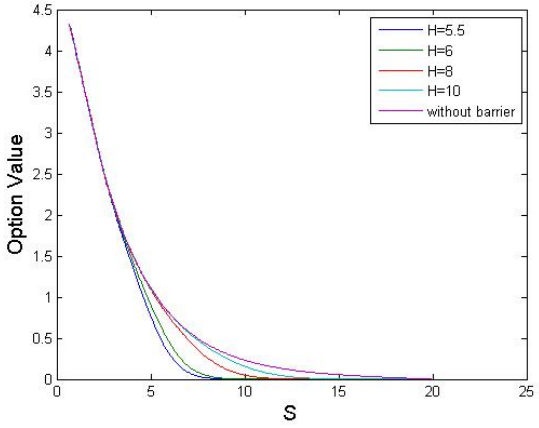

Figure 4.9: The influence of the discrete barrier on the American put option price. The barriers discretely monitored at 10 monitoring dates, where H=[5.5, 6, 8, 10].

the barrier moves outward, Delta becomes flatter and approaches to the shape of a regular American option. We also find that Gamma has the highest value between S=2 and S=3, which is the region of free boundary. Moreover, for each case, Gamma also gives high values around its barriers.

4.4.4 Other Hedge Ratios of American Discrete Barrier Option

This subsection studies the hedge ratios of Rho and Vega for American Discrete Barrier Options.

The Greek Rho

Consider an American put option with knock-out barrier H=6 which has 10 monitoring dates, volatility=40%, and interest rates 5%, 7%, 9%, 11%, 13%, 15%. Figure 4.12 illustrates the Greek Rho with interest rate= 7%, 9%, 11%, 13%. We notice that all Rho are negative, which tells us that the put option value is negatively correlated to the interest rates. Furthermore, Rho has higher absolute value when interest is smaller, meaning that the option has higher sensitivity when the interest rate is small. It also suggests that the option value is more sensitive when the underlying asset price is close to the strike price, while less sensitive when it is deep in the money or deep out of the money. Moreover,

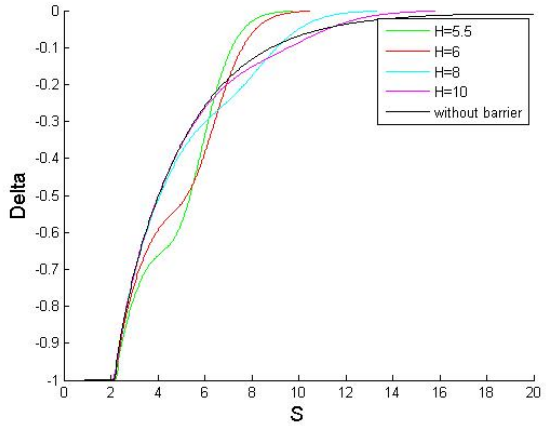

Figure 4.10: The influence of the barrier on the value of Delta for the American discrete barrier options.

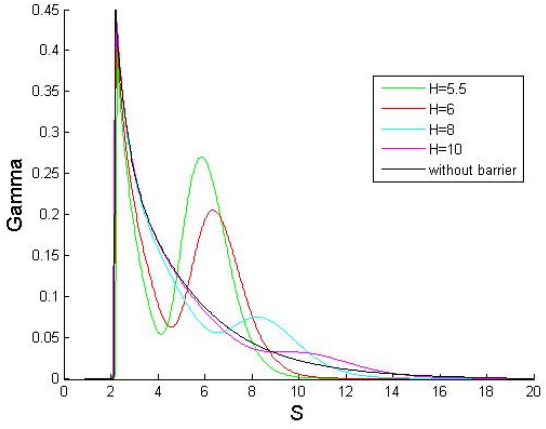

Figure 4.11: Influence of the barrier on the value of Gamma for American discrete barrier options.

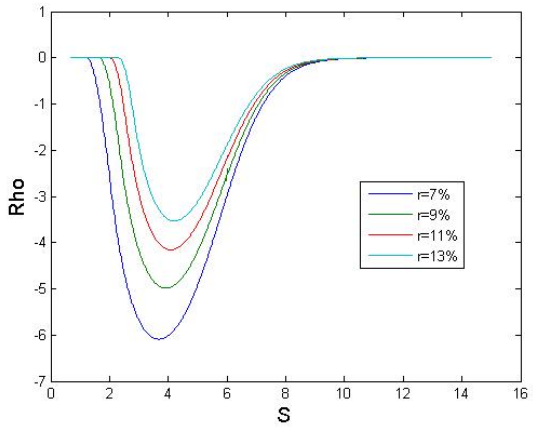

Figure 4.12: The value of Rho for American discrete barrier options.

we notice the phase shift of Rho which means that when the interest rate increases, the maximum point of Rho is shifted to the right. This probably results from the effect of the barrier.

The Greek Vega

We take an American put option with knock-out barrier H=6 which has 10 monitoring dates, and volatility=20%, 30%, 40%, 50%, 60%. Figure 4.13 shows the value of Vega for the discrete barrier option. We find that all the value of Vega are positive, which means that the option value is positively correlated to the volatility. We also notice that in the case of lower volatility, the sensitivity of the option value is higher when it is at the money, while lower when it is deep in the money or deep out of the money.

4.5 Conclusions

In this Chapter we investigated the projected successive over-relaxation scheme, the penalty scheme, the Brennan Schwartz scheme and the explicit front fixing scheme when applied to pricing American put options. These finite differences schemes have been shown to be able to obtain accurate solutions for American options. We found that, in case of one dimensional

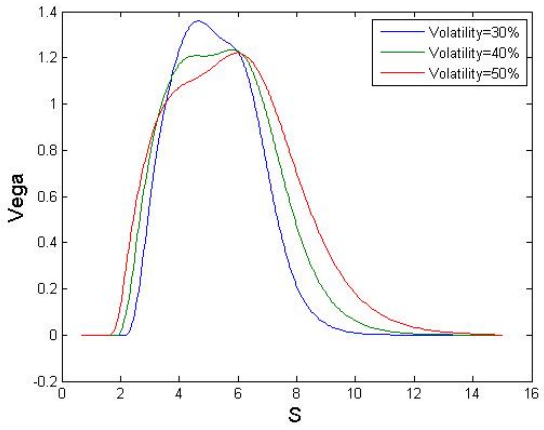

Figure 4.13: The value of Vega for American discrete barrier options.

American option models, when using a small number of grid points, the Brennan Schwartz scheme and the explicit front tracking scheme are good candidates which spend less CPU time, while the penalty scheme outperforms as the number of grid points increases.

For solving higher dimensional American option models, the penalty scheme seemed to be more flexible and efficient, since modern large sparse algebraic solvers, such as BiCGstab or CGS, can be applied. Although the Brennan Schwartz scheme performs well in the one dimensional case, it is not a good choice in higher dimensional models.

In order to give insight into hedging American options, we did several numerical simulations to further study the hedge factors for American options with continuous and discrete monitoring barrier.

Chapter 5

Conclusion

There are four ways of determining the arbitrage-free value of the option: 1) Analytic and approximation solutions; 2) Binomial tree method; 3) Monte Carlo simulation; 4) Partial differential equation framework. The PDE option pricing framework has a faster convergence and has the advantage of providing the entire option value surface as well as the hedge factors, which can be useful for risk management.

In this project, we investigated the application of finite difference schemes to option pricing problems, especially the barrier option and American option pricing problems. For the purpose of comparison, a Monte Carlo method and a binomial tree method are also implemented for pricing barrier options and American options.

In the case of barrier options, the Black-Scholes equation involves discontinuities, which is known to cause difficulties in obtaining accurate results. To deal with this difficulty, we introduced a new adaptive mesh method. We not only implemented the adaptive mesh method for continuous barrier options but also extended it to cases when the barrier is discretely monitored and the barrier is time dependent. The big advantage of this method is that the mesh nodes are relocated in the regions which involve large numerical errors, which will reduce the global error substantially. The algorithm automatically selects the grid by using a moving mesh solver, which ran for a coarse mesh and obtained the structure of the solution for an option model. The method has been tested successfully for problems with three different types of barrier options. The adaptive mesh method combines the merit of the moving mesh method and the efficiency of fixed mesh methods. It is able to obtain more accurate solutions without taking much additional computational time. By using the adaptive mesh method, we also did several numerical simulations to give insight into to the

price and hedge of discrete barrier options.

In the case of American options, we investigated several finite difference methods, i.e., the projected successive over-relaxation scheme, the penalty scheme, the Brennan Schwartz scheme and the explicit front fixing scheme. During several tests, these finite differences schemes have shown to be capable tools for pricing American options. Moreover, we found that for one-dimensional American option models, when using a small number of grid points, the Brennan Schwartz scheme and the explicit front tracking scheme are good candidates which spend less CPU time, while the penalty scheme outperforms as the number of grid points increases. For solving higher dimensional American option models, the penalty methods seemed to be more flexible and efficient, since modern large sparse algebraic solvers, such as BiCGstab or CGS, can be applied. Although the Brennan Schwartz scheme performs well in the one-dimensional case, it is not a good choice in higher dimensional models. Finally, to give insight into finite difference numerical methods to price and hedge American options, we did several numerical simulations for hedging factors of American put options with barriers.

5.1 Suggestions for Future Research

Finding an optimized adaption function, which gives a good measure of numerical error distribution, still offers potential for further improvements regarding accuracy. It would be of great interest to know how the adaptive mesh method applies to American exotic options models. It is also interesting to further investigate the performance of adaptive mesh methods for higher dimensional problems and jump-diffusion models.

Bibliography

[1] F. Black and M. Scholes. The pricing of options and corporate liabilities. *Journal of Political Economy*, 81(3), May 9 2001.

[2] P.P. Boyle. Options: A monte carlo approach. *J. Fin. Econ.*, (4):323–338, 1977.

[3] P.P. Boyle. A lattice framework for option pricing with two state variables. *The Journal of Financial and Quantitative Analysis*, 23(1):1–12, 1988.

[4] P.P. Boyle and Y. Tian. An explicit finite difference approach to the pricing of barrier options. *Applied Mathematical Finance*, 5(6):17–43, 3/1998.

[5] M. Brennan and E. Schwartz. The valuation of American put options. *Journal of Finance*, 32:449–462, 1977.

[6] M. Broadie, P. Glasserman, and S.G. Kou. A continuity correction for discrete barrier options. *Journal of Mathematical Finance*, 1997.

[7] M. Broadie and Y. Yamamoto. A double-exponential fast Gauss transform algorithm for pricing discrete path-dependent options. *Oper. Res.*, 53(5):764–779, 2005.

[8] Peter Carr. Randomization and the American put. *The Review of Financial Studies*, 11(3):597–626, 1998.

[9] Don M. Chance. *Analysis of Derivatives for the CFA Program*. 2003.

[10] N. Clarke and K. Parrott. Multigrid for American option pricing with stochastic volatility. *Applied Mathematical Finance*, 6:177–195(19), 1 September 1999.

[11] F. Coman. An iterative method for pring the American put options with dividends. Master's thesis, University of British Columbia, 2005.

[12] J.C. Cox, S.A. Ross, and M. Rubinstein. Option pricing: A simplified approach. *J. Fin. Econ.*, 7(6):229–263, 1979.

[13] J.D. Evans, R. Kuske, and Joseph B. Keller. American options of assets with dividends near expiry. *Math. Finance*, 12(3):219–237, 2002.

[14] S. Figlewski and B. Gao. The adaptive mesh model: A new approach to efficient option pricing. *J. Fin. Econ.*, 53(3):313–351, 1999.

[15] P. A. Forsyth and K. R. Vetzal. Quadratic convergence for valuing American options using a penalty method. *SIAM J. Sci. Comput.*, 23(6):2095–2122 (electronic), 2002.

[16] B. Giovanni and R.E. Whaley. Efficient analytic approximation of american option values. *The Journal of Finance*, 42(2):301–320, 1987.

[17] H. Han and X. Wu. A fast numerical method for the Black-Scholes equation of American options. *SIAM J. NUMER. ANAL.*, 41(6):2081–2095, 2003.

[18] E.G. Haug. *The Complete Guide to Option Pricing Formulas*. McGraw-Hill, New York, U.S.A., 2006.

[19] M.E. Hosea and L.F. Shampine. Analysis and implementation of tr-bdf2. *Appl. Numer. Math.*, 20(1-2):21–37, 1996.

[20] J. Huang and J. Pang. Option pricing and linear complementarity. *J. Comput. Fin.*, 2(3), 1998.

[21] J. Huang, M.G. Subrahmanyam, and G.G. Yu. Pricing and hedging American options: A recursive integration method. *The Review of Financial Studies*, 9(1):277–300, 1996.

[22] W. Huang, Y. Ren, and R.D. Russell. Moving mesh partial differential equations (MMPDES) based on the equidistribution principle. *SIAM J. Numer. Anal.*, 31(3):709–730, 1994.

[23] W. Huang and R.D. Russell. Analysis of moving mesh partial differential equations with spatial smoothing. *SIAM J. Numer. Anal.*, 34(3):1106–1126, 1997.

[24] John Hull. *Options, Futures, and Other Derivatives*. Fifth edition, 2003.

[25] P. Jaillet, D. Lamberton, and B. Lapeyre. Variational inequalities and the pricing of American options. *Acta Appl. Math.*, 21(3):263–289, 1990.

[26] L. Jiang and M. Dai. Convergence of binomial tree methods for European/American path-dependent options. *SIAM J. Numer. Anal.*, 42(3):1094–1109 (electronic), 2004.

[27] L. Jiang and C. Li. *Mathematical Modeling and Methods of Option Pricing*. World Scientific Publishing Company, 2005.

[28] F. A. Longstaff and E. S. Schwartz. Valuing American options by simulation: A simple least-squares approach. *Journal of Finance*, May 9 2001.

[29] Robert C. Merton. Theory of rational option pricing. *Bell J. Econom. and Management Sci.*, 4:141–183, 1973.

[30] S. Metwally and A. Atiya. Using brownian bridge for fast simulation of jump-diffusion processes and barrier options. *Journal of Derivatives*, Fall 2002.

[31] B.F. Nielsen, O. Skavhaug, and A. Tveito. A penalty scheme for solving American option problems. In *Progress in industrial mathematics at ECMI 2000 (Palermo)*, volume 1 of *Math. Ind.*, pages 608–612. Springer, Berlin, 2002.

[32] B.F. Nielsen, O. Skavhaug, and A. Tveito. A penalty scheme for solving American option problems. In *Progress in industrial mathematics at ECMI 2000 (Palermo)*, volume 1 of *Math. Ind.*, pages 608–612. Springer, Berlin, 2002.

[33] D. M. Pooley, K. R. Vetzal, and P. A. Forsyth. Convergence remedies for non-smooth payoffs in option pricing. *J. Comput. Fin.*, 6:25–40, 2003.

[34] E. Reiner and M. Rubinstein. Breaking down the barriers. *Risk*, (4):28–35, 1991.

[35] Peter Sonneveld. Cgs: A fast Lanczos-type solver for nonsymmetric linear systems. *SIAM J. Sci. Stat. Comput.*, 10(1):36–52, 1989.

[36] A. Tagliani. Discrete monitored barrier options by finite difference schemes. Technical Report 38100, Faculty of Economics, Trento University, Trento, Italy.

[37] D. Tavella and C. Randall. *Pricing Financial Instruments: The Finite Difference Method*. John Wiley and Sons, New York, U.S.A., 2000.

[38] H.A. van der Vorst. Bi-cgstab: a fast and smoothly converging variant of bi-cg for the solution of nonsymmetric linear systems. *SIAM J. Sci. Stat. Comput.*, 13(2):631–644, 1992.

[39] K.R. Vetzal and P.A. Forsyth. Discrete parisian and delayed barrier options: A general numerical approach. *Adv. Futures Options Research*, 10:1–16, 1999.

[40] P. Wilmott, J. Dewynne, and S. Howison. *Option Pricing: Mathematical Models and Computation*. Oxford Financial Press, Oxford, UK, 1995.

[41] L. Wu and Y.K. Kwok. A front-fixing finite difference method for the valuation of American options. *J. Fin. Eng.*, 6(2):83–97, 1997.

[42] Y. Zhu, X. Wu, and I. Chen. *Derivatives Securities and Difference Methods*. Springer, fifth edition, 2004.

[43] R. Zvan, P.A. Forsyth, and K.R. Vetzal. Penalty methods for American options with stochastic volatility. *J. Comput. Appl. Math.*, 91(2):199–218, 1998.

[44] R. Zvan, K.R. Vetzal, and P.A. Forsyth. PDE methods for pricing barrier options. *J. Econom. Dynam. Control*, 24(11-12):1563–1590, 2000. Computational aspects of complex securities.

[45] R. Zvan, K.R. Vetzal, and P.A. Forsyth. PDE methods for pricing barrier options. *J. Econ. Dyn. Con.*, 24:1563–1590, 2000.